

## Discontinuity factors in SP3 theory

*Master's Thesis in Nuclear Engineering*

MIKAEL ANDERSSON

Department of Applied Physics  
*Division of Nuclear Engineering*  
CHALMERS UNIVERSITY OF TECHNOLOGY  
Gothenburg, Sweden 2011  
CTH-NT-246

ISSN 1653-4662



CTH-NT-246

# Discontinuity factors in SP3 theory

Master's Thesis in Nuclear Engineering  
MIKAEL ANDERSSON

Department of Applied Physics  
*Division of Nuclear Engineering*  
CHALMERS UNIVERSITY OF TECHNOLOGY  
Gothenburg, Sweden 2011

Discontinuity factors in SP3 theory  
MIKAEL ANDERSSON

CTH-NT-246  
ISSN 1653-4662  
Department of Applied Physics  
Division of Nuclear Engineering  
Chalmers University of Technology  
SE-412 96 Gothenburg  
Sweden  
Telephone: + 46 (0)31-772 1000

Cover:

The front image shows the heterogeneous (solid) and homogeneous (dashed) fluxes calculated in this thesis for the BWR example.

Chalmers Reproservice  
Gothenburg, Sweden 2011

Discontinuity factors in SP3 theory

Master's Thesis in Nuclear Engineering

MIKAEL ANDERSSON

Department of Applied Physics

Division of Nuclear Engineering

Chalmers University of Technology

Keywords: Neutronics, Homogenization, Diffusion, SP3, Discontinuity factors

## Abstract

The SP3 theory is a better approximation than diffusion theory when modeling a nuclear reactor, but the properties of homogenization and discontinuity factors are not known.

This master thesis, at Studsvik Scandpower, has been done to investigate the usage of discontinuity factors in the SP3 theory and compare the results with the traditional diffusion theory. The discontinuity factors should have the property to conserve the reaction rates and interface currents.

Four different methods were tested to create discontinuity factors for SP3 theory, one analytical and three numerical. Two methods (the analytical one and one of the numerical methods) were able to conserve both the currents and reaction rates but at different costs. The analytical method has the problem of possible numerical instabilities, and the numerical method the problem of no unique solution. Good approximations are also found with minimal errors in flux and the effective multiplication factor  $k_{eff}$ .

The thesis has shown that it is possible to use discontinuity factors in SP3 theory, either by recreating the solution completely, or use good approximations. For more reliable results and numerical stabilities some future improvements are needed.

As a good approximation found was to use the traditional discontinuity factors with the change that the discontinuity factors for the second moment flux is set to unity.

## Abstract

SP3 approximationen är ett bättre sätt att modelera en kärnreaktor än den nu använda diffusions teorin, men när det gäller homogenisering och diskontinuitets faktorer är detta ännu inte testat.

Detta examensarbete har gjorts på Studsvik Scandpower för att undersöka diskontinuitetsfaktorer i SP3 teori och jämföra resultaten med den traditionella diffusionsteorin. Det som kommer att krävas av diskontinuitetsfaktorerna är att de ska bevara antalet reaktioner och läckage.

För att göra detta har fyra olika metoder testats för att beräkna diskontinuitetsfaktorer för SP3 teori, en analytisk och tre numeriska metoder. Två metoder, den analytiska och en av de numeriska, klarade av att skapa diskontinuitetsfaktorer som bevarade de önskade storheterna, men inte utan problem. Problemet med den analytiska metoden är att det kan uppstå numeriska instabiliteter och den numeriska metoden har problemet att det inte finns en unik lösning. En approximation har även hittats med små fel i såväl flöde och  $k_{eff}$ .

Examensarbetet har visat att det är möjligt att använda diskontinuitetsfaktorer i SP3 teori, antingen genom att återskapa lösningen eller med approximationer. För att få mer pålitliga resultat och numerisk stabilitet behövs fler förbättringar.

Den bästa approximationen som hittats i detta arbete var att använda de traditionella diskontinuitetsfaktorer med ändringen att diskontinuitetsfaktorerna för andra ordningens flöde sätts till ett.



## Acknowledgment

First of all I would like to thank my supervisor Sten-Örjan Lindahl at Studsvik Scandpower who has helped me and guided me through this thesis. My examiner Imre Pázsit and the others at the department of nuclear engineering at Chalmers, for their help and support. Ivar Gustavsson at the department of mathematical sciences. For the moral support I would like to thank my family and friends.

## Abbreviations and notations

In this report the conventional subscripts for the fast and thermal groups  $_1, _2$  will not be used, this is because of 1 and 2 will have other meanings with SP3 equations. Therefore the subscripts for the fast group will be  $_f$  and for thermal  $_t$ , i.e. the fast and thermal fluxes will be called  $\phi_f \phi_t$ .

Otherwise the following conventional physical quantities will be used:

|                     |   |  |
|---------------------|---|--|
| $\phi_g$            | - | scalar flux of group g                 |
| $J$                 | - | neutron current                        |
| $j$                 | - | partial neutron current                |
| $\Sigma_\alpha$     | - | cross-section                          |
| $D_g$               | - | diffusion coefficient                  |
| $\nu_g$             | - | number of neutrons released in fission |
| $\Sigma_{a,g}$      | - | absorption cross-section               |
| $\Sigma_{f,g}$      | - | fission cross-section                  |
| $\Sigma_{s,gg'}$    | - | scattering cross-section               |
| $k_{eff}$           | - | effective multiplication factor        |
| $\bar{\phantom{x}}$ | - | average quantity                       |
| PWR                 | - | pressurized water reactor              |
| BWR                 | - | boiling water reactor                  |
| MOX                 | - | Mixed oxide                            |

And to clarify, in this report vectors will be written as bold  $\phi$  and matrices as bold with an underline  $\underline{\Sigma}$ .

# Contents

|   |           |
|---|-----------|
| Acknowledgment . . . . .                                | II        |
| Abbreviations and notations . . . . .                   | III       |
| <b>1 Introduction</b>                                   | <b>1</b>  |
| 1.1 Background . . . . .                                | 1         |
| 1.2 Purpose . . . . .                                   | 2         |
| 1.3 Studsvik Scandpower . . . . .                       | 2         |
| 1.4 Report outline . . . . .                            | 2         |
| <b>2 Theory</b>   | <b>3</b>  |
| 2.1 Neutron transport . . . . .                         | 3         |
| 2.1.1 Energy groups . . . . .                           | 3         |
| 2.1.2 Nodalization . . . . .                            | 4         |
| 2.1.3 Angular approximations . . . . .                  | 5         |
| 2.1.3.1 Diffusion approximation . . . . .               | 5         |
| 2.1.3.2 Simplified P3 approximation, SP3 . . . . .      | 5         |
| 2.2 Boundary conditions . . . . .                       | 7         |
| 2.2.1 Diffusion . . . . .                               | 7         |
| 2.2.2 SP3 . . . . .                                     | 8         |
| 2.3 Heterogeneous system . . . . .                      | 8         |
| 2.4 Homogenization . . . . .                            | 8         |
| 2.5 Discontinuity factors . . . . .                     | 9         |
| <b>3 Numerical methods</b>                              | <b>11</b> |
| 3.1 Numerical calculations . . . . .                    | 11        |
| 3.1.1 Numerical method . . . . .                        | 11        |
| 3.1.2 Implementation of Discontinuity factors . . . . . | 13        |
| 3.2 Discontinuity factors for SP3 theory . . . . .      | 13        |
| 3.2.1 Method 1 - Traditional definition . . . . .       | 14        |
| 3.2.2 Method 2 - Nodal optimization . . . . .           | 15        |
| 3.2.3 Method 3 - Interface optimization . . . . .       | 16        |
| 3.2.4 Method 4 -Core optimization . . . . .             | 17        |
| 3.3 The code . . . . .                                  | 18        |
| 3.4 Materials and example systems . . . . .             | 20        |

---

|          |  |           |
|----------|--|-----------|
| 3.4.1    | Materials . . . . .  | 20        |
| 3.4.2    | Example system . . . . .   | 21        |
| 3.5      | Albedo calculations . . . . .                                    | 22        |
| <b>4</b> | <b>Results</b>   | <b>24</b> |
| 4.1      | Heterogeneous solution . . . . .                                 | 24        |
| 4.1.1    | Diffusion . . . . .  | 24        |
| 4.1.2    | SP3 . . . . .  | 25        |
| 4.2      | Homogeneous solution . . . . .                                   | 25        |
| 4.2.1    | Homogeneous solution from heterogeneous solution . . . . .       | 26        |
| 4.2.1.1  | Diffusion . . . . .  | 26        |
| 4.2.1.2  | SP3 . . . . .  | 26        |
| 4.2.2    | Homogeneous solution from discontinuity factors . . . . .        | 27        |
| 4.2.2.1  | Error calculations . . . . .                                     | 28        |
| 4.2.2.2  | Discontinuity factors . . . . .                                  | 29        |
| 4.3      | Albedo calculations . . . . .                                    | 31        |
| <b>5</b> | <b>Discussion</b>  | <b>33</b> |
| 5.1      | Result comparisons . . . . .                                     | 33        |
| 5.2      | Methods . . . . .  | 33        |
| 5.2.1    | Method 1 . . . . .   | 34        |
| 5.2.2    | Method 2 . . . . .   | 34        |
| 5.2.3    | Method 4 . . . . .   | 34        |
| 5.3      | Albedo calculation . . . . .                                     | 35        |
| <b>6</b> | <b>Conclusion and Future work</b>                                | <b>36</b> |
| <b>A</b> | <b>Matrix form of transport equations</b>                        | <b>38</b> |
| A.1      | Diffusion . . . . .  | 38        |
| A.2      | SP3 . . . . .  | 38        |
| <b>B</b> | <b>Derivations</b>   | <b>40</b> |
| B.1      | Nodal solution with known average flux and<br>currents . . . . . | 40        |
| B.2      | Nodal solution with known interface fluxes . . . . .             | 43        |
| B.3      | Albedo tests . . . . .   | 45        |

# Chapter 1

## Introduction

### 1.1 Background

When modeling a nuclear reactor, the neutron flux is one of the most important parameters to calculate. Today there are a number of codes available to do this, but since a nuclear reactor is a very complex system it is impossible to solve the equations describing the neutron flux exactly and approximations are necessary.

To be able to calculate the neutron flux, there are approximations made about energy-, space-, and angular-dependence. To handle the angular dependence the so called diffusion approximation is applied. In some cases the simplified P3 (SP3) theory is applied, since it is known that the SP3 equations is a much better approximation than diffusion, especially when come to mixed oxide fuel (MOX) [BL00].

The space dependence is taken care of by homogenization of the core in a couple of steps, from pin cell, assembly and core level, in the final step the core is divided into homogeneous “cubes”. One problem with the homogenization is that it will give rise to discontinuities at the “cube” interfaces [Dem10].

With the diffusion approximation these discontinuities can be handled with so called discontinuity factors and the parameters of interest can be recreated. The problem with SP3 theory is that the properties of discontinuity factors have not been investigated for SP3 theory yet.

## 1.2 Purpose

The tasks defined for this thesis are

- to derive a method to compute discontinuity factors for the SP3 equations. These discontinuity factors shall have the property of preserving the neutron balance, i.e. reaction rates and node leakages, for each node and group.
- to perform numerical investigation in 1D for a number of typical PWR and BWR configurations. Of special interest will be to compare traditional P1 discontinuity factors with the new SP3 ones.

An additional task was to compare how the used boundary conditions changes when SP3 theory is used compared with diffusion theory.

## 1.3 Studsvik Scandpower

Studsvik Scandpower is the provider of a wide range of analysis tools for nuclear reactors eg. Simulate 5 and Casmo 5 amongst others. Studsvik softwares are the most widely used software for light water reactors. Studsvik Scandpower is situated in United States, Sweden, Norway, Switzerland, Germany and Japan, and has almost 50 engineers employed [Sca11].

## 1.4 Report outline

This report will start with a briefing of the most important theory, concepts and equations needed for the thesis. The following chapter will present the theory for the SP3 equations and the numerical tools used to solve the problem. The subsequent chapters will present the results from the numerical investigations, and discussion around them.

# Chapter 2

## Theory

### 2.1 Neutron transport

The neutron balance in a reactor can be represented by the neutron transport equation, also called the linear Boltzmann equation. This is a very complicated equation and will not be treated in this thesis, but equations derived from it will be used. To be able to see why some of the approximations are needed it can be good to see it.

Since no time dependencies will be of interest in this thesis the time independent transport equation is sufficient to study

$$\begin{aligned} & \boldsymbol{\Omega} \cdot \nabla \psi(\mathbf{r}, \boldsymbol{\Omega}, E) + \Sigma_T(\mathbf{r}, E) \psi(\mathbf{r}, \boldsymbol{\Omega}, E) \\ &= \int_{(4\pi)} \int_0^\infty \Sigma_s(\mathbf{r}, \boldsymbol{\Omega}' \rightarrow \boldsymbol{\Omega}, E' \rightarrow E) \psi(\mathbf{r}, \boldsymbol{\Omega}', E') d\omega' dE' \\ &+ \frac{\chi(E)}{4\pi} \int_0^\infty \nu(E') \Sigma_f(\mathbf{r}, E') \phi(\mathbf{r}, E') dE' \end{aligned} \tag{2.1}$$

This equation is not possible to solve, except in some simple cases, but by making some approximations it becomes manageable. Some of these approximations are discussed briefly below, more about these approximations can be seen in [Dem10]

#### 2.1.1 Energy groups

Since the dependence of energy within all cross-sections ( $\Sigma$ ) is very complicated, as can be seen in Figure 2.1, the transport equation (2.1) is divided into energy groups. Then the energy integrals in (2.1) will be calculated over these energy groups and new energy averaged  $\Sigma_\alpha$  will be created. The scattering cross-section  $\Sigma_s$  will be divided into new  $\Sigma_{s,gg}$  (self-scattering cross-sections) and  $\Sigma_{s,gg'}$  (down and up scattering cross-sections), which will be used instead [Dem10]. In this thesis two energy groups will be used, “fast” and “thermal”, and will be discussed more later on.

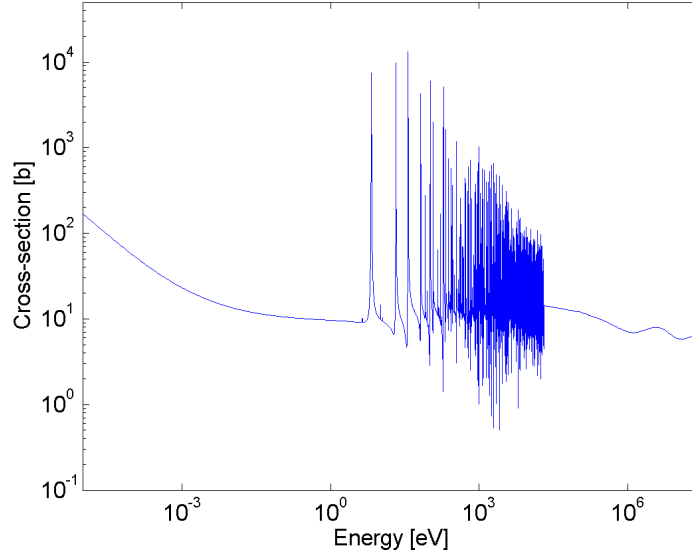


**Figure 2.1** - Total cross-section of  $^{238}_{92}\text{U}$ , nuclear data collected from [Cha11].

### 2.1.2 Nodalization

To handle the space dependence of the cross-sections (and later on the diffusion coefficient), the total volume  $V$  is divided into sub nodes  $V_i$ , which has constant cross-sections, in other words  $\Sigma(\mathbf{r}) = \Sigma_i$ .

This can be done in small geometries, but in a full size reactor this is impossible. To handle this a couple of sub nodes are gathered into a node  $V_I$ , this will be more discussed in Section 2.4

For each and one of these nodes and energy groups the so called continuity equation (2.2) needs to be satisfied [Dem10].

$$\sum_{i=1}^S \frac{1}{h_i} J_g + (\Sigma_{a,g} + \Sigma_{r,g}) \bar{\phi}_g - \frac{1}{k_{eff}} \sum_{g'=1}^G \nu_{g'} \Sigma_{f,g'} \bar{\phi}_{g'} - \sum_{\substack{g'=1 \\ g' \neq g}}^G \Sigma_{s,gg'} \bar{\phi}_{g'} = 0 \quad (2.2)$$

where  $h_i$  is the node size,  $S$  is the number of surface interfaces to other nodes, in 1 dimension  $S = 2$ , and  $G$  is the number of energy groups. Equation (2.2) can be written in matrix form as follows

$$\sum_{i=1}^S \frac{1}{h_i} \mathbf{J} - \underline{\Sigma} \bar{\phi} = 0 \quad (2.3)$$

### 2.1.3 Angular approximations

The goal of this thesis is to compare two different approximations concerning the angular dependence of the flux. An approximation of the angular dependence is needed because of the angular dependent scattering integral in (2.1). This together with the energy group approximation will lead to new cross-sections that handle scattering within and between groups, called  $\Sigma_{s,gg'}$ .

The angular approximation used in this thesis is the  $P_N$  approximation also called spherical harmonics, where  $N$  represents the order of spherical harmonics used. The two used are the P1 and SP3, where S stands for simplified. Derivations of the multi group P1 equations which leads to the diffusion equation and the SP3 equations can be seen in [LMM96], [BL00] and [Dem10].

#### 2.1.3.1 Diffusion approximation

With the approximations discussed earlier the one dimensional two group diffusion equations can be written as

$$\begin{aligned} D_f \frac{\partial^2}{\partial x^2} \phi_f - (\Sigma_{a,f} + \Sigma_{s,tf}) \phi_f + \frac{1}{k_{eff}} (\nu_t \Sigma_{f,f} \phi_f + \nu_t \Sigma_{f,t} \phi_t) + \Sigma_{s,ft} \phi_t &= 0 \\ D_t \frac{\partial^2}{\partial x^2} \phi_t - (\Sigma_{a,t} + \Sigma_{s,ft}) \phi_t + \Sigma_{s,t} \phi_f &= 0 \end{aligned} \quad (2.4)$$

To make equation 2.4 more easily implemented in a computer code it can be written in matrix form

$$\underline{D} \frac{\partial^2}{\partial x^2} \underline{\phi} + \underline{\Sigma} \underline{\phi} = 0 \quad (2.5)$$

more about this in Section A.1

#### 2.1.3.2 Simplified P3 approximation, SP3

The SP3 approximation will give rise to one additional flux  $\phi_g^{(2)}$  called the second moment flux. This is the second moment of the Legendre expansion and therefore one additional equation for each group is needed. The one dimensional two group SP3 equations can be written as

$$\begin{aligned}
D_{1,f} \frac{\partial^2}{\partial x^2} \Phi_f - \Sigma_{r1,f} \phi_f^{(0)} + Q_f &= 0 \\
D_{3,f} \frac{\partial^2}{\partial x^2} \phi_f^{(2)} - \Sigma_{r3,f} \phi_f^{(2)} + \frac{2}{3} [\Sigma_{r1,f} \phi_f^{(0)} - Q_f] &= 0 \\
D_{1,t} \frac{\partial^2}{\partial x^2} \Phi_t - \Sigma_{r1,t} \phi_t^{(0)} + Q_t &= 0 \\
D_{3,t} \frac{\partial^2}{\partial x^2} \phi_t^{(2)} - \Sigma_{r3,t} \phi_t^{(2)} + \frac{2}{3} [\Sigma_{r1,t} \phi_t^{(0)} - Q_t] &= 0 \\
Q_f = \frac{1}{k_{eff}} [\nu_t \Sigma_{f,f} \phi_f^{(0)} + \nu_t \Sigma_{f,t} \phi_t^{(0)}] + \Sigma_{s,ft} \phi_t^{(0)} \\
Q_t = \Sigma_{s,t} \phi_f^{(0)}
\end{aligned} \tag{2.6}$$

where the scalar flux  $\Phi_g$  is defined as

$$\Phi_g = \phi_g^{(0)} + 2\phi_g^{(2)} \tag{2.7}$$

and the new cross-sections is defined as

$$\begin{aligned}
\Sigma_{r1,g} &= \Sigma_{a,g} + \Sigma_{s,g'g} \\
\Sigma_{r3,g} &= \frac{5}{3} (\Sigma_{r1,g} + \Sigma_{s,gg}) \\
D_{3,g} &= \frac{3}{7(\Sigma_{r1,g} + \Sigma_{s,gg})}
\end{aligned} \tag{2.8}$$

To make equation (2.6) more manageable they are rewritten with the relation in equation (2.7) to

$$\begin{aligned}
D_{1,f} \frac{\partial^2}{\partial x^2} \Phi_f - \Sigma_{r1,f} \Phi_f + Q_f + 2\Sigma_{r1,f} \phi_f^{(2)} &= 0 \\
D_{3,f} \frac{\partial^2}{\partial x^2} \phi_f^{(2)} - \Sigma_{r3,f} \phi_f^{(2)} + \frac{2}{3} [\Sigma_{r1,f} (\Phi_f - 2\phi_f^{(2)}) - Q_f] &= 0 \\
D_{1,t} \frac{\partial^2}{\partial x^2} \Phi_t - \Sigma_{r1,t} \Phi_t + Q_t + 2\Sigma_{r1,t} \phi_t^{(2)} &= 0 \\
D_{3,t} \frac{\partial^2}{\partial x^2} \phi_t^{(2)} - \Sigma_{r3,t} \phi_t^{(2)} + \frac{2}{3} [\Sigma_{r1,t} (\Phi_t - 2\phi_t^{(2)}) - Q_t] &= 0 \\
Q_f = \frac{1}{k_{eff}} [\nu_t \Sigma_{f,f} (\Phi_f - 2\phi_f^{(2)}) + \nu_t \Sigma_{f,t} (\Phi_t - 2\phi_t^{(2)})] + \Sigma_{s,ft} (\Phi_t - 2\phi_t^{(2)}) \\
Q_t = \Sigma_{s,t} (\Phi_f - 2\phi_f^{(2)})
\end{aligned} \tag{2.9}$$

One needs to keep in mind that the integral flux is  $\phi_g^{(0)}$  (the flux comparable with  $\phi_g$  in the diffusion theory), not  $\Phi_g$  which only is a mathematical tool, which is the flux of interest. Since the SP3 equations (2.9) can be seen as an expansion of the diffusion

equation (2.4), and by inserting  $\phi_g^{(2)} = 0$  in (2.9) the diffusion equation (2.4) is obtained. As in the diffusion case equation (2.9) will be written on matrix form

$$\underline{D} \frac{\partial^2}{\partial x^2} \phi + \underline{\Sigma} \phi = 0 \quad (2.10)$$

more about this in Section A.2

## 2.2 Boundary conditions

To be able to solve the differential equation (2.10) boundary conditions are needed. There are some different boundary conditions that are applied in these kind of problems, in this thesis the albedo boundary condition will be applied.

The albedo works with the partial currents  $j^+$  (out of the core) and  $j^-$  (back to the core) with the following relation

$$j^- = \underline{a} j^+ \quad (2.11)$$

where  $\underline{a}$  is the albedo matrix.

To have a total reflective boundary i.e. all neutrons are reflected back to the core,  $\underline{a} = \underline{I}$  where  $\underline{I}$  is the identity matrix. To have a “black” boundary i.e. no neutrons are reflected, the albedo matrix will be a zero matrix  $\underline{a} = \underline{0}$ .

### 2.2.1 Diffusion

The partial currents in diffusion theory is defined as [Dem10]

$$\begin{aligned} j^+ &= \frac{1}{4} \phi_s + \frac{1}{2} J \\ j^- &= \frac{1}{4} \phi_s - \frac{1}{2} J \end{aligned} \quad (2.12)$$

where  $\phi_s$  is the interface flux.

By using the partial currents (for every group) in equation (2.12) and the albedo equation (2.11) a relation of the boundary current can be derived

$$\underline{J} = \frac{1}{2} (\underline{I} + \underline{a})^{-1} (\underline{I} - \underline{a}) \phi_s \quad (2.13)$$

Equation (2.13) will be used as boundary condition.

### 2.2.2 SP3

In similar manner the partial currents for the SP3 equations is defined as [BL00]

$$\begin{aligned}
 j_1^+ &= \frac{1}{4}\phi_s^{(0)} + \frac{1}{2}J_1 - \frac{3}{16}\phi_s^{(2)} \\
 j_1^- &= \frac{1}{4}\phi_s^{(0)} - \frac{1}{2}J_1 - \frac{3}{16}\phi_s^{(2)} \\
 j_3^+ &= \frac{5}{16}\phi_s^{(2)} + \frac{1}{2}J_3 - \frac{1}{16}\phi_s^{(0)} \\
 j_3^- &= \frac{5}{16}\phi_s^{(2)} - \frac{1}{2}J_3 - \frac{1}{16}\phi_s^{(0)}
 \end{aligned} \tag{2.14}$$

To include  $\Phi$  instead of  $\phi^{(0)}$  equation (2.7) is used in equation (2.14) and the partial currents are written as

$$\begin{aligned}
 j_1^+ &= \frac{1}{4}\Phi_s + \frac{1}{2}J_1 - \frac{11}{16}\phi_s^{(2)} \\
 j_1^- &= \frac{1}{4}\Phi_s - \frac{1}{2}J_1 - \frac{11}{16}\phi_s^{(2)} \\
 j_3^+ &= \frac{7}{16}\phi_s^{(2)} + \frac{1}{2}J_3 - \frac{1}{16}\Phi_s \\
 j_3^- &= \frac{7}{16}\phi_s^{(2)} - \frac{1}{2}J_3 - \frac{1}{16}\Phi_s
 \end{aligned} \tag{2.15}$$

by using equation (2.15) and the albedo (2.11) the boundary current can be derived as

$$\mathbf{J} = \frac{1}{2}(\mathbf{I} + \mathbf{a})^{-1}(\mathbf{I} - \mathbf{a})\mathbf{B}\phi_s \tag{2.16}$$

where  $\mathbf{B}$  for two groups is defined as

$$\mathbf{B} = \begin{bmatrix} 1 & \frac{-11}{4} & 0 & 0 \\ \frac{-1}{4} & \frac{7}{4} & 0 & 0 \\ 0 & 0 & 1 & \frac{-11}{4} \\ 0 & 0 & \frac{-1}{4} & \frac{7}{4} \end{bmatrix} \tag{2.17}$$

## 2.3 Heterogeneous system

When this approximations are made the system can more easily be solved. The SP3 or diffusion equation will then be needed to be solved in each sub node, and with the boundary condition that the flux  $\phi$  and the neutron current  $J$  should be continuous in between nodes. More about this in Section 3.1.1.

As an example core in 1-D, study Figure 2.2, where each node  $n$  is composed of different sub nodes  $m$  which has a set of constant cross-sections.

## 2.4 Homogenization

When the heterogeneous system has been solved, a homogenization can be made for each node, to gather the sub nodes (m) into nodes (n) see Figure 2.2. The new homogeneous

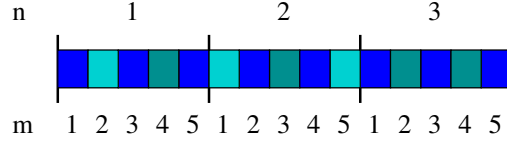


**Figure 2.2** - An example of a core,  $n$  denotes the nodes and  $m$  the sub nodes. Blue fields represents water and gray fields represents fuel or other materials.

cross-sections are calculated with the heterogeneous flux as a weight as [Dem10]

$$\Sigma_{\alpha,g}^{hom} = \frac{\int_{V_I} \Sigma_{\alpha,g}(\mathbf{r}) \phi_g(\mathbf{r}) dV}{\int_{V_I} \phi_g(\mathbf{r}) dV} \quad (2.18)$$

In the SP3 case there are different fluxes to use but since  $\phi^{(0)}$  is the integral flux, this is used for homogenization as shown in equation (2.19). Why the coefficients for  $\phi^{(2)}$  also can be weighted with  $\phi^{(0)}$  is because they are defined from the same cross-sections as  $\phi^{(0)}$  and there are no new cross-section specific for the equations concerning  $\phi^{(2)}$ , as shown in equation (2.8).

$$\Sigma_{\alpha,g}^{hom} = \frac{\int_{V_I} \Sigma_{\alpha,g}(\mathbf{r}) \phi_g^{(0)}(\mathbf{r}) dV}{\int_{V_I} \phi_g^{(0)}(\mathbf{r}) dV} \quad (2.19)$$

Since the cross-sections now are changed, the homogeneous flux  $\phi^{hom}$  will not be the same as the heterogeneous flux. There will therefore be some constraints on the homogeneous flux  $\phi^{hom}$  [Dem10] the first is conservation of reaction rates

$$\int_{V_I} \Sigma_{\alpha,g}(\mathbf{r}) \phi_g(\mathbf{r}) dV = \int_{V_I} \Sigma_{\alpha,g}^{hom} \phi_g^{hom} dV \quad (2.20)$$

and the second is the interface currents at interface  $k$

$$\int_{S_I^k} \mathbf{J}_g \cdot \mathbf{n} dS = \int_{S_I^k} \mathbf{J}_g^{hom} \cdot \mathbf{n} dS \quad (2.21)$$

## 2.5 Discontinuity factors

The constraints on the homogeneous flux are to keep the most important aspects of the heterogeneous system, but one thing that will not be conserved with this homogenization is the interface flux in between two nodes, one example can be seen in Figure 2.3. In diffusion theory this problem is handled with discontinuity factors defined as [Dem10]

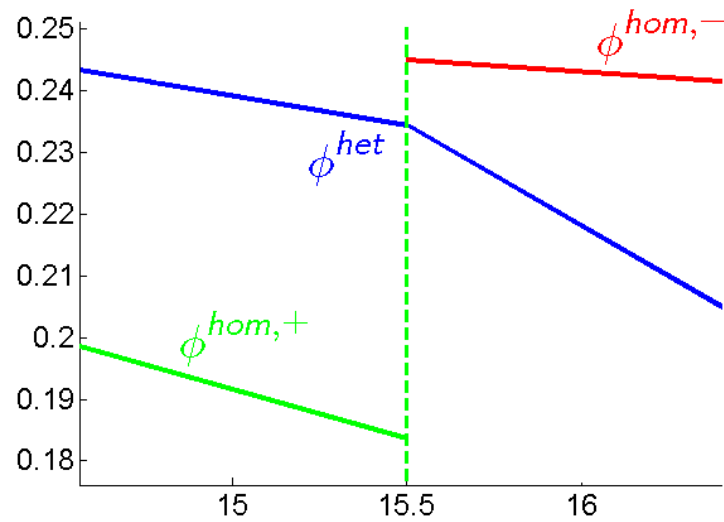


**Figure 2.3** - An example of the homogeneous and heterogeneous solutions at a node interface.

$$f_{n,g}^{\pm} = \frac{\phi_{n,g}^{het\pm}}{\phi_{n,g}^{hom\pm}} \quad (2.22)$$

Since there are two different homogeneous fluxes at each interface it will create two different discontinuity factors for each interface and node, see Figure 2.3. With these discontinuity factors the conservation restraints set in equations (2.20) and (2.21) will be fulfilled.

# Chapter 3

## Numerical methods

### 3.1 Numerical calculations

To solve the task given, computer codes were written in MatLab. In this thesis only a one dimensional slab reactor was investigated. Since the thesis was to test the theory, one dimension is sufficient and the results can easily be generalized into two or three dimensions. In one dimension it is possible to solve the system exactly and therefore no additional approximations will be needed. The limit of the solution will be how many decimals required from the numerical solver.

#### 3.1.1 Numerical method

For each homogeneous node in one dimension an exact solution can be given (see Appendix B for derivations). It is only necessary to get the average flux  $\bar{\phi}$  to get the reaction rates, neutron currents at the interface  $J$ , interface fluxes  $\phi_{nm}$  and the effective multiplication factor  $k_{eff}$ . The interface current is given by

$$\mathbf{J}^+ = -\underline{\mathbf{d}}(\phi^+ - \underline{\mathbf{s}}\bar{\phi}) \quad (3.1)$$

where the definitions of  $\underline{\mathbf{d}}$  and  $\underline{\mathbf{s}}$  can be found in equation (B.27) in Appendix B. However the current  $J$  can be expressed with only average fluxes

$$\mathbf{J}_{n \rightarrow m} = \underline{\mathbf{C}}_{nm}\bar{\phi}_n - \underline{\mathbf{C}}_{mn}\bar{\phi}_m \quad (3.2)$$

where

$$\underline{\mathbf{C}}_{nm} = (\underline{\mathbf{d}}_n^{-1} + \underline{\mathbf{d}}_m^{-1})^{-1} \underline{\mathbf{s}}_n \quad (3.3)$$

By using the requirement that the heterogeneous flux and the net current are continuous, one may derive

$$-\underline{\mathbf{C}}_{n-1,n}\bar{\phi}_{n-1} + (\underline{\mathbf{C}}_{n,n-1} + \underline{\mathbf{C}}_{n,n+1} - h\underline{\Sigma}_n)\bar{\phi}_n - \underline{\mathbf{C}}_{n+1,n}\bar{\phi}_{n+1} = 0 \quad (3.4)$$

The boundary conditions in equation (2.16) and (2.13) gives a relation for the current  $\mathbf{J}$ . Then a new  $\underline{\mathbf{d}}$  matrix will be defined in the diffusion case as

$$\underline{\mathbf{d}}_{ref} = \frac{1}{2}(\underline{\mathbf{I}} + \underline{\mathbf{a}})^{-1}(\underline{\mathbf{I}} - \underline{\mathbf{a}}) \quad (3.5)$$

and in the SP3 case

$$\underline{\mathbf{d}}_{ref} = \frac{1}{2}(\underline{\mathbf{I}} + \underline{\mathbf{a}})^{-1}(\underline{\mathbf{I}} - \underline{\mathbf{a}})\underline{\mathbf{B}} \quad (3.6)$$

By solving the system in equation (3.4) the average flux  $\bar{\phi}$  can be found for every node in the system. The side currents can be found by equation (3.2) and the side fluxes by

$$\phi_{nm} = \underline{\mathbf{d}}_m^{-1}\underline{\mathbf{C}}_{nm}\bar{\phi}_n - \underline{\mathbf{d}}_n^{-1}\underline{\mathbf{C}}_{mn}\bar{\phi}_m \quad (3.7)$$

derivations can be found in Section B.1.

Equation (3.4) can not be solved directly since it is an eigenvalue equation for  $k_{eff}$ , which can be seen in the definition of the cross-section matrix

$$\underline{\Sigma}_n = \underline{\Sigma}_{a_n} + \underline{\Sigma}_{s_n} + \frac{1}{k_{eff}}\underline{\Sigma}_{f_n} \quad (3.8)$$

To solve for both  $\bar{\phi}$  and  $k_{eff}$  in (3.4) an iterative method is used. The parameter that contains  $k_{eff}$  is set as a ‘‘source term’’ on the right hand side, add the superscript  $t$  (an iteration parameter) and (3.4) can be rewritten as

$$-\underline{\mathbf{C}}_{n-1,n}^{t-1}\bar{\phi}_{n-1}^t + (\underline{\mathbf{C}}_{n,n-1}^{t-1} + \underline{\mathbf{C}}_{n,n+1}^{t-1} - h\underline{\Sigma}_n^*)\bar{\phi}_n^t - \underline{\mathbf{C}}_{n+1,n}^{t-1}\bar{\phi}_{n+1}^t = \frac{1}{k_{eff}^{t-1}}\underline{\Sigma}_{f_n}\bar{\phi}_n^{t-1} \quad (3.9)$$

where  $\underline{\Sigma}_n^* = \underline{\Sigma}_{a_n} + \underline{\Sigma}_{s_n}$ .

A start guess ( $t = 0$ ) is then needed for the flux  $\bar{\phi}^0$  and  $k_{eff}^0$ , in this thesis the start guess is set to 1 for all values. The  $\underline{\mathbf{C}}^0$  matrices is calculated with the start guess for  $k_{eff}^0$  and a new flux  $\bar{\phi}^1$  can be calculated by solving the system in equation (3.9). The  $k_{eff}^1$  is updated with

$$k_{eff}^t = k_{eff}^{t-1} \frac{(\underline{\Sigma}_{f_n}\bar{\phi}_n^{t-1}) \cdot (\underline{\Sigma}_{f_n}\bar{\phi}_n^t)}{(\underline{\Sigma}_{f_n}\bar{\phi}_n^{t-1}) \cdot (\underline{\Sigma}_{f_n}\bar{\phi}_n^{t-1})} \quad (3.10)$$

With a new  $k_{eff}^t$  new  $\underline{\mathbf{C}}^t$  can be calculated (see Section B.1). With new  $\underline{\mathbf{C}}^t$  equation (3.9) is updated and the procedure repeats. These iterations called power iterations are carried out until the change in  $k_{eff}$  is at a desired level, in this thesis  $10^{-10}$ . More about this methodology and derivations in [Dem10].

### 3.1.2 Implementation of Discontinuity factors

To implement the discontinuity factors one can study

$$\mathbf{J}^{hom+} = -\underline{\mathbf{d}}(\phi^{hom+} - \underline{\mathbf{s}}\bar{\phi}^{hom}) \quad (3.11)$$

Since both  $\mathbf{J}^+$  and  $\bar{\phi}$  is controlled by the constraints in equation (2.20) and (2.21), the only parameter changing from the heterogeneous system to the homogeneous is  $\underline{\mathbf{d}}$ ,  $\underline{\mathbf{s}}$  and the interface flux  $\phi^+$ . With the definition of discontinuity factors in equation (2.22), containing the homogeneous and heterogeneous interface flux, equation (3.11) can be rewritten to

$$\mathbf{J}^{hom+} = -\underline{\mathbf{d}}(\underline{\mathbf{f}}^{-1}\phi^{het+} - \underline{\mathbf{s}}\bar{\phi}^{hom}) \quad (3.12)$$

where  $\underline{\mathbf{f}}$  is a diagonal matrix with the discontinuity factors. To include  $\underline{\mathbf{f}}$  in the  $\underline{\mathbf{d}}$  and  $\underline{\mathbf{s}}$  matrices equation (3.12) can be written as

$$\mathbf{J}^{hom+} = -\underline{\mathbf{d}}_f(\phi^{het+} - \underline{\mathbf{s}}_f\bar{\phi}^{hom+}) \quad (3.13)$$

where

$$\begin{aligned} \underline{\mathbf{d}}_f &= \underline{\mathbf{d}}\underline{\mathbf{f}}^{-1} \\ \underline{\mathbf{s}}_f &= \underline{\mathbf{f}}\underline{\mathbf{s}} \end{aligned} \quad (3.14)$$

The system can now be solved with the same principle as in Section 3.1.1, but with new matrices  $\underline{\mathbf{d}}_f$  and  $\underline{\mathbf{s}}_f$ , two different for each node [Lin11].

## 3.2 Discontinuity factors for SP3 theory

Since the task is to investigate the discontinuity factors for the SP3 equations different definitions and methods are tested. The definitions are made for the system shown in equation (2.9) ie.  $\Phi_g$  and  $\phi_g^{(2)}$  were used. The discontinuity factors for  $\Phi_g$  is called  $f_{n,g}^{(0)\pm}$  and  $\phi_g^{(2)}$  is called  $f_{n,g}^{(2)\pm}$ .

In method 2, 3 and 4 the goal is to put  $f_{n,g}^{(2)\pm} = 1$ , so that no extra parameters needs to be added, and still satisfy the conservation equation (2.3) for the integral flux, the properties for the second moment flux (reaction rates and interface current will not be considered). The numerical solver used is *fsolve* in MatLab which chooses the best algorithm for the given problem.

### 3.2.1 Method 1 - Traditional definition

The first method tested was to define the discontinuity factors as in equation (2.22) but an additional one for  $\phi_g^{(2)}$  as

$$f_{n,g}^{(0)\pm} = \frac{\Phi_{n,g}^{het\pm}}{\Phi_{n,g}^{hom\pm}} \quad (3.15)$$

$$f_{n,g}^{(2)\pm} = \frac{\phi_{n,g}^{(2)het\pm}}{\phi_{n,g}^{(2)hom\pm}} \quad (3.16)$$

where the heterogeneous interface flux  $\phi_n^{het\pm}$  is taken from the heterogeneous solution calculated with equation (3.7) and the homogeneous interface flux  $\phi_n^{hom\pm}$  is calculated by some manipulation of equation (3.1), the same equation holds for  $\mathbf{J}^-$  and  $\phi^-$ . By this the homogeneous interface flux can be calculated by

$$\begin{aligned} \phi^{hom+} &= -\underline{\mathbf{d}}^{-1} \mathbf{J}^+ + \underline{\mathbf{s}} \bar{\phi}^{hom} \\ \phi^{hom-} &= -\underline{\mathbf{d}}^{-1} \mathbf{J}^- + \underline{\mathbf{s}} \bar{\phi}^{hom} \end{aligned} \quad (3.17)$$

the currents are taken from the heterogeneous solution since of the conservation equation (2.21), and the homogeneous average flux is calculated with

$$\bar{\phi}^{hom} = \frac{1}{h} \sum_{i=1}^m \bar{\phi}_i^{het} dV \quad (3.18)$$

the parameters that changes in equation (3.17) are the matrices  $\underline{\mathbf{d}}$  and  $\underline{\mathbf{s}}$  since these are found from the cross-sections (see Section B.1). This method is expected to be functional since it is an extension of the theory from diffusion theory.

Two different variations were tested for this method. The first was to use the same discontinuity factors for the integral flux  $f_{n,g}^{(0)\pm}$  as in equation (3.17) and use  $f_{n,g}^{(2)\pm} = 1$ . The second variation was to use the discontinuity factors calculated from the diffusion theory as  $f_{n,g}^{(0)\pm}$  and use  $f_{n,g}^{(2)\pm} = 1$ . These are not expected to recreate the true solution but are investigated how good approximations they are.

### 3.2.2 Method 2 - Nodal optimization

This method is based on solving the diffusion or SP3 equations with known interface fluxes for one node. For a more illustrative view of the system, see Figure 3.1 and for derivations see Section B.2.

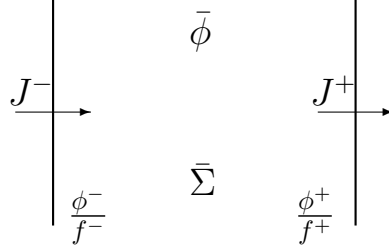


**Figure 3.1** - The domain for solving with the nodal optimization.

This way of solving for each node will result in expressions for the current and the average flux as

$$\begin{aligned} \mathbf{J}^{\pm} &= \frac{2}{h} \underline{\mathbf{D}}^* \underline{\mathbf{C}} \underline{\mathbf{U}}^* \phi_s \\ \bar{\phi} &= \underline{\mathbf{U}} \underline{\mathbf{M}}^* \underline{\mathbf{U}}^* \phi_s \end{aligned} \quad (3.19)$$

where  $\phi_s$  for the two group SP3 equation is defined as

$$\phi_s = \left[ \Phi_f^- \quad \phi_f^{(2)-} \quad \Phi_t^- \quad \phi_t^{(2)-} \quad \Phi_f^+ \quad \phi_f^{(2)+} \quad \Phi_t^+ \quad \phi_t^{(2)+} \right]^T \quad (3.20)$$

the definitions of  $\underline{\mathbf{D}}^*$ ,  $\underline{\mathbf{C}}$ ,  $\underline{\mathbf{U}}^*$ ,  $\underline{\mathbf{U}}$  and  $\underline{\mathbf{M}}^*$  can be found in Appendix B.2 equation (B.46), it should be noted that this method will have problems when the buckling  $b_i \rightarrow 0$ , but since only the method is tested this is not handled.

Instead of defining  $\phi_s$  as in equation (3.20) the discontinuity factors are included and define

$$\phi_s = \left[ \frac{\Phi_f^-}{f_f^{(0)-}} \quad \frac{\phi_f^{(2)-}}{f_f^{(2)-}} \quad \frac{\Phi_t^-}{f_t^{(0)-}} \quad \frac{\phi_t^{(2)-}}{f_t^{(2)-}} \quad \frac{\Phi_f^+}{f_f^{(0)+}} \quad \frac{\phi_f^{(2)+}}{f_f^{(2)+}} \quad \frac{\Phi_t^+}{f_t^{(0)+}} \quad \frac{\phi_t^{(2)+}}{f_t^{(2)+}} \right]^T \quad (3.21)$$

By fix all  $f_2^{\pm} = 1$  equation (3.21) can be written as

$$\phi_s = \left[ \frac{\Phi_f^-}{f_f^{(0)-}} \quad \phi_f^{(2)-} \quad \frac{\Phi_t^-}{f_t^{(0)-}} \quad \phi_t^{(2)-} \quad \frac{\Phi_f^+}{f_f^{(0)+}} \quad \phi_f^{(2)+} \quad \frac{\Phi_t^+}{f_t^{(0)+}} \quad \phi_t^{(2)+} \right]^T \quad (3.22)$$

All interface fluxes  $\Phi_g^{\pm}$  and  $\phi_g^{(2)\pm}$  are known from the heterogeneous solution, calculated with equation (3.7). Since the quantities needs to be conserved, the current  $\mathbf{J}^{\pm}$  and average flux  $\bar{\phi}$  (from reaction rates) is taken from the heterogeneous solution and the equations that will be solved to get the new discontinuity factors are

$$\begin{aligned} \mathbf{J}^{hom\pm}(f) - \mathbf{J}^{het\pm} &= 0 \\ \bar{\phi}^{hom}(f) - \bar{\phi}^{het} &= 0 \end{aligned} \quad (3.23)$$

In equation (3.23) the homogeneous current and average flux is calculated by equation (3.19) and the discontinuity factors  $f_f^{(0)-}$ ,  $f_t^{(0)-}$ ,  $f_f^{(0)+}$  and  $f_t^{(0)+}$  are optimized to fulfill equation (3.23).

It can be noted that for diffusion theory this method will not require a numerical solution since it can be solved exact.

### 3.2.3 Method 3 - Interface optimization

The average flux  $\bar{\phi}_g$  can be used as input in equation (3.2) and (3.7) to get the interface current  $\mathbf{J}_{nm}$  and interface flux  $\phi_{nm}$  in between to neighbor nodes, see Figure 3.2.

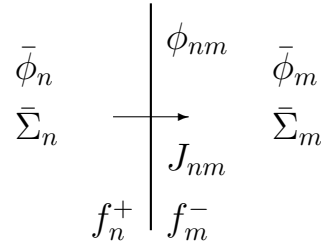


**Figure 3.2** - The domain for solving with the interface optimization.

By applying discontinuity factors (as done in Section 3.1.2) to get the new relations

$$\begin{aligned} \mathbf{J}_{n \rightarrow m} &= \underline{\mathbf{C}}_{nm}^n \bar{\phi}_n - \underline{\mathbf{C}}_{mn}^m \bar{\phi}_m \\ \phi_{nm} &= (\underline{\mathbf{d}}_m(\underline{\mathbf{f}}_m^-)^{-1})^{-1} \underline{\mathbf{C}}_{nm}^n \bar{\phi}_n - (\underline{\mathbf{d}}_n(\underline{\mathbf{f}}_n^+)^{-1})^{-1} \underline{\mathbf{C}}_{mn}^m \bar{\phi}_m \end{aligned} \quad (3.24)$$

where

$$\begin{aligned} \underline{\mathbf{C}}_{nm}^n &= [(\underline{\mathbf{d}}_n(\underline{\mathbf{f}}_n^+)^{-1})^{-1} + (\underline{\mathbf{d}}_m(\underline{\mathbf{f}}_m^-)^{-1})^{-1}]^{-1} \underline{\mathbf{f}}_n^- \underline{\mathbf{s}}_n \\ \underline{\mathbf{C}}_{nm}^m &= [(\underline{\mathbf{d}}_n(\underline{\mathbf{f}}_n^+)^{-1})^{-1} + (\underline{\mathbf{d}}_m(\underline{\mathbf{f}}_m^-)^{-1})^{-1}]^{-1} \underline{\mathbf{f}}_m^+ \underline{\mathbf{s}}_m \end{aligned} \quad (3.25)$$

and for two group SP3 equation

$$\underline{\mathbf{f}}_n^\pm = \begin{bmatrix} f_{n,f}^{(0)\pm} & 0 & 0 & 0 \\ 0 & f_{n,f}^{(2)\pm} & 0 & 0 \\ 0 & 0 & f_{n,t}^{(0)\pm} & 0 \\ 0 & 0 & 0 & f_{n,t}^{(2)\pm} \end{bmatrix} \quad (3.26)$$

and by fixing  $f_{g,2}^{\pm} = 1$  leads to

$$\underline{\mathbf{f}}_n^{\pm} = \begin{bmatrix} f_{n,f}^{(0)\pm} & 0 & 0 & 0 \\ 0 & 1 & 0 & 0 \\ 0 & 0 & f_{n,t}^{(0)\pm} & 0 \\ 0 & 0 & 0 & 1 \end{bmatrix} \quad (3.27)$$

Since the average flux  $\bar{\phi}$  is known from the reaction rates for each node calculated by equation (3.18), and the current and interface fluxes are taken from the heterogeneous solution and the equations that will be solved to get the new discontinuity factors are

$$\begin{aligned} \mathbf{J}_{nm}^{hom\pm}(f) - \mathbf{J}_{nm}^{hom\pm} &= 0 \\ \phi_{nm}^{hom}(f) - \phi_{nm}^{het} &= 0 \end{aligned} \quad (3.28)$$

where the homogeneous current and interface flux are calculated by equation (3.24). The discontinuity factors  $f_{n,f}^{(0)+}$ ,  $f_{n,t}^{(0)+}$ ,  $f_{n,f}^{(0)-}$  and  $f_{n,t}^{(0)-}$  are optimized to fulfill equation (3.28).

### 3.2.4 Method 4 -Core optimization

The core optimization solves the entire homogeneous system with discontinuity factors, this means that the system of equations in equation (3.4) is solved with the  $\underline{\mathbf{C}}$  matrices calculated with discontinuity factors as in equation (3.14), and the same iterative solver as in Section 3.1.1. An overview can be seen in Figure 3.3. This is the same program that tests the discontinuity factors in the end of the thesis, see Section 3.3.

Since the hole system is used this method will be tested with different sets of equations to optimize, containing the heterogeneous average flux  $\bar{\phi}_n$ , currents  $\mathbf{J}_N$  and interface flux  $\phi_N$ , see Table 3.1. As in method 2 and 3 the discontinuity factors in method 4 are used to fulfill the equations given in Table 3.1.

**Table 3.1** - The different tests in method 4, optimization variables refers to the unknowns in the system and equations refers to the equations used in the optimization.

| Test | optimization variables | Equations   |
|------|------------------------|---|
| 1    | $f_{n,g}^{(0)\pm}$     | $\mathbf{J}_N^{hom} - \mathbf{J}_N^{het} = 0$<br>$\bar{\phi}_n^{hom} - \bar{\phi}_n^{het} = 0$                                      |
| 2    | $f_{n,g}^{(0)\pm}$     | $\mathbf{J}_n^{hom} - \mathbf{J}_n^{het} = 0$<br>$\bar{\phi}_n^{hom} - \bar{\phi}_n^{het} = 0$<br>$\phi_N^{hom} - \phi_N^{het} = 0$ |

This method is likely to work since all conservations are taken under consideration when solving the system. To ensure that the solver does not find a local minimum, different start guesses will be tested.

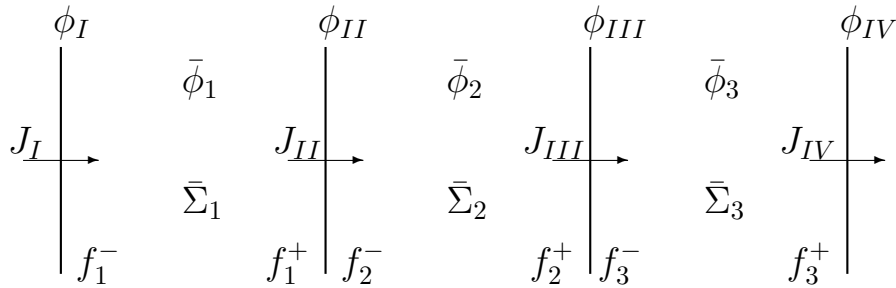


**Figure 3.3** - The domain for solving with the core optimization.

### 3.3 The code

The main code developed was to solve the linear system in equation (3.9) for a given geometry  $(n, m, comp)$ , cross-section data  $(\Sigma_\alpha)$  boundary conditions  $(\underline{a})$  and the error criterion for  $k_{eff}$  called  $k_{err}$ , and return the average flux  $(\bar{\phi})$ , interface current  $(\mathbf{J})$  and interface fluxes  $(\phi^\pm)$  for all nodes in the system and the effective multiplication factor  $(k_{eff})$  for the whole system.

The heterogeneous average flux calculated was used to calculate the new homogeneous cross-sections  $(\Sigma_\alpha^{hom})$ , and homogeneous average flux  $(\bar{\phi}^{hom})$ . The discontinuity factors  $(f^\pm)$  was calculated using the different methods defined in Section 3.2. One last program was used to calculate the homogeneous flux  $(\bar{\phi}^{hom})$ , the interface currents  $(\mathbf{J}^{hom})$  and the effective multiplication factor  $(k_{eff}^{hom})$  using the homogeneous cross-sections  $(\Sigma_\alpha^{hom})$ , discontinuity factors  $(f^\pm)$  and the other same boundary conditions  $(\underline{a})$  as in the heterogeneous system. The heterogeneous and the homogeneous results were compared to evaluate the methods to calculate the discontinuity factors. An overview of the calculation scheme can be seen in Figure 3.4.

**Validations** To have some validation of the results two tests were implemented in the solver. The first test was the continuity equation (2.3) and it was tested for each sub node to ensure that the correct solution was given. The second test was to check that the boundary condition was satisfied. This was done by calculating the partial currents as in equation (2.13) and (2.16), and use the partial currents in the albedo relation (2.11) to verify that it was fulfilled. At last the  $k_{eff}$  was compared with an existing code provided by the supervisor.

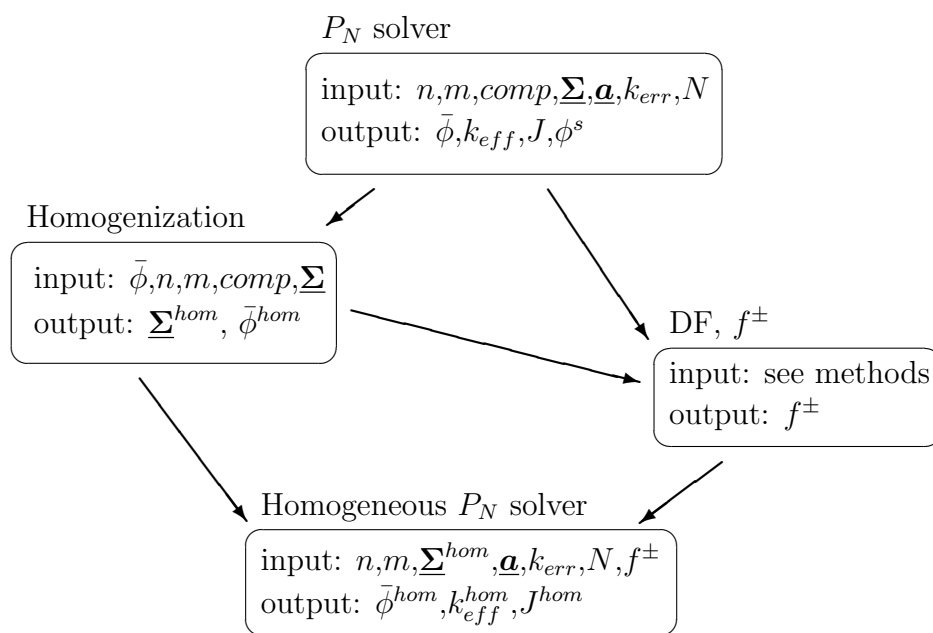


**Figure 3.4** - Calculation scheme. Input data is defined as:  $n$  - number of nodes,  $m$  - number of sub nodes,  $comp$  - composition of the core,  $\underline{\Sigma}$  - cross-sections,  $\underline{a}$  - albedo matrices for both boundaries,  $k_{err}$  - maximum error in  $k_{eff}$  (end of iterations) and  $N - 1$  for diffusion or 3 for SP3.

## 3.4 Materials and example systems

There are a number of different materials in a nuclear reactor. The main materials in a nuclear reactor are the fuel, coolant and moderator. But there are also building materials and materials controlling the reactivity. The materials used in this thesis will be briefly discussed below.

### 3.4.1 Materials

There are two main types of fuel used in commercial reactors today, uranium oxide (UOX) and mixed oxide (MOX) [CLR02].

**Uranium oxide** The UOX is the most common fuel type in the world's nuclear reactors today. It consists of  $\text{UO}_2$  with an atomic fraction of 3-4%  $^{235}\text{U}$  and 96-97%  $^{238}\text{U}$ . The fissile material in this kind of fuel is  $^{235}\text{U}$  and later on in the cycle even plutonium (both  $^{239}\text{Pu}$  and  $^{241}\text{Pu}$ ) will be present due to transmutation of  $^{238}\text{U}$  [CLR02].

**Mixed oxide** MOX is a mixture of plutonium oxide and uranium oxide either natural or depleted. Since plutonium is not a natural element this type of fuel can only be made either by recycling of used nuclear fuel [CLR02] or decommissioning of nuclear weapons [BRL95].

**Differences** There are some crucial difference between UOX and MOX fuels, both concerning safety and neutronics. In the neutronics case, the MOX fuel has a higher absorption cross-section than UOX, see Figure 3.5, and this results in a much lower thermal flux [BRL95]. The interface between UOX and MOX fuel will have big changes due to the difference in thermal flux and the diffusion approximation may have problems with this behavior [FCM95]. From the safety point of view MOX fuel will result in less delayed neutrons and therefore increase the risk of prompt criticality and risk of hot spots [Tre06].

**Moderator** The moderator is a material that is good for slowing down neutrons to thermal energies, since the neutrons is "born" fast but the highest cross-section for fission is in the thermal region, see Figure 3.5. The most common moderator is light water and it works as a coolant as well, these reactors are called light water reactors. Other used moderators is heavy water<sup>1</sup> (CANDU reactors) and graphite (RBMK) [CLR02].

**Absorbers** Different reactors have different methods to control the reactivity and to shut down the reactor. In a BWR there can be two different types of reactivity control, control rods (CR) and burnable absorbers, sometimes called burnable poison. The PWR uses dissolved boron in the moderator as reactivity control.

---

<sup>1</sup>water containing  $^2\text{H}$

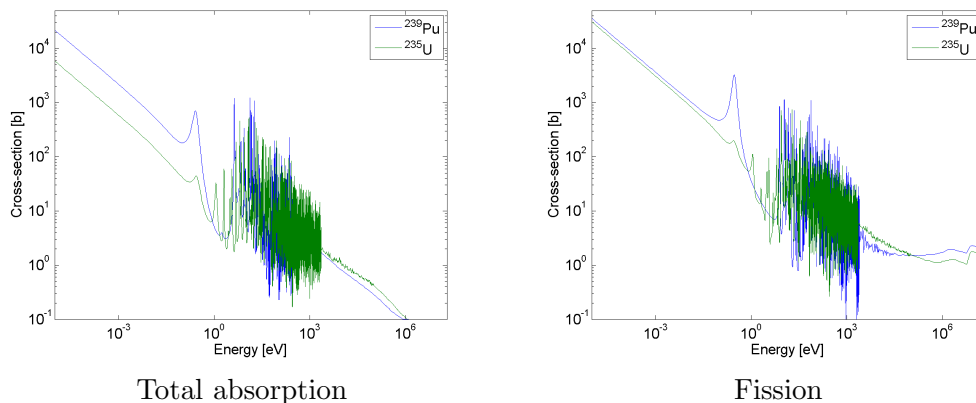


**Figure 3.5** - Different cross-sections for  $^{235}_{92}\text{U}$  and  $^{239}_{94}\text{Pu}$ , nuclear data collected from [Cha11].

The control rods consists of boron where  $^{10}\text{B}$  has a high cross-section for the  $(n,\alpha)$  reaction and thereby absorbs neutrons. As burnable absorbers gadolinium is used, and it has a high cross-section for the  $(n,\gamma)$  reaction [Dem09] [Cha11].

### 3.4.2 Example system

Two different example systems were investigated, one with PWR pin cross-section data and one with BWR pin cross-section data. The materials used can be seen in Table 3.2, cross-sections for the different materials were calculated with CASMO 5 and was provided by the supervisor, the cross-sections can be seen in Table 3.2.

The PWR system contains both UOX and MOX fuel, the boundary conditions was set to reflective. The system was divided into three homogeneous parts of equal size, two for the UOX fuel and one for the MOX fuel. The geometry of the PWR system can be seen in Figure 3.6.

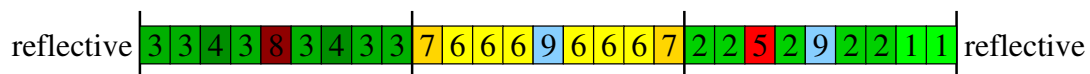


**Figure 3.6** - The example PWR core, all nodes are 2 cm wide. The materials can be seen in Table 3.2.

The BWR system is a UOX system, with different enrichment, the boundary conditions was set to reflective at the left boundary and a moderator as the right boundary condition, this means an “infinite amount of water” as boundary. The geometry of the BWR system can be seen in Figure 3.7. As in the PWR example the BWR example was divided in to three homogeneous parts.

Both systems have control rods and burnable absorbers in form of gadolinium present.



**Figure 3.7** - The example BWR core, all nodes are 2 cm wide except the ones with a \* that are 1 cm, the materials can be seen in Table 3.2.

**Table 3.2** - Materials and cross-sections used in example cores, 6/3 % refers to 6 % Gd and 3% enriched UOX

| No | Material<br>(enrichment) | $D_f$              | $\Sigma_{a,f}$       | $\nu\Sigma_{f,f}$    | $\Sigma_{s,ff}$      | $\Sigma_{s,ft}$      |
|----|--------------------------|--------------------|----------------------|----------------------|----------------------|----------------------|
|    |                          | $D_t$              | $\Sigma_{a,t}$       | $\nu\Sigma_{f,t}$    | $\Sigma_{s,tf}$      | $\Sigma_{s,tt}$      |
| 1  | UOX (0.7%)               | 1.45216<br>0.43179 | 0.008143<br>0.038111 | 0.003426<br>0.038103 | 0.480757<br>0.015590 | 0.000873<br>1.093845 |
| 2  | UOX (2%)                 | 1.45758<br>0.43427 | 0.009226<br>0.066008 | 0.005513<br>0.098705 | 0.478997<br>0.014744 | 0.001450<br>1.075212 |
| 3  | UOX (3%)                 | 1.46111<br>0.43380 | 0.009992<br>0.084777 | 0.006997<br>0.139163 | 0.477793<br>0.014160 | 0.001821<br>1.065544 |
| 4  | UOX (5%)                 | 1.46768<br>0.42960 | 0.011376<br>0.117665 | 0.009702<br>0.209558 | 0.475527<br>0.013126 | 0.002435<br>1.053462 |
| 5  | Gd/UOX (6/3%)            | 1.46456<br>0.38038 | 0.013919<br>0.382798 | 0.006141<br>0.038650 | 0.476514<br>0.010971 | 0.006886<br>1.076887 |
| 6  | MOX (3%)                 | 1.47720<br>0.38419 | 0.011350<br>0.200539 | 0.007733<br>0.338973 | 0.475318<br>0.012764 | 0.003903<br>1.074907 |
| 7  | MOX (5%)                 | 1.48474<br>0.36249 | 0.012732<br>0.273780 | 0.010343<br>0.474706 | 0.473141<br>0.011718 | 0.004990<br>1.078224 |
| 8  | Control rod (CR)         | 1.43310<br>0.23607 | 0.038283<br>0.720099 | 0.000000<br>0.000000 | 0.463088<br>0.006038 | 0.003356<br>1.149276 |
| 9  | Water                    | 1.80019<br>0.33291 | 0.000330<br>0.008137 | 0.000000<br>0.000000 | 0.572272<br>0.028793 | 0.001245<br>1.639387 |

### 3.5 Albedo calculations

Since the moderator in the BWR example is in form of water, the albedo matrix for water needs to be calculated. To calculate the albedo matrix the diffusion equation and the SP3 equations are solved for a reflector that is infinite thick (derivations and definitions can be seen in Appendix B Section B.3), then a relation for the albedo matrix can be found as

$$\underline{a} = -(\underline{G}\underline{U}\underline{b}\underline{U}^{-1}\underline{D}^{-1} + \frac{1}{2}\underline{I})^{-1}(\frac{1}{2}\underline{I} - \underline{G}\underline{U}\underline{b}\underline{U}^{-1}\underline{D}^{-1}) \quad (3.29)$$

where  $\underline{G}$  is a matrix that is different for diffusion and SP3 and  $\underline{U}$ ,  $\underline{b}$  and  $\underline{D}$  are material (in this case water) matrices.

To test this a simple example was set, seen in Figure 3.8. One reference calculation was carried out using a large number of water nodes, enough nodes so that the flux is  $\approx 0$ , and one calculation with the calculated albedo matrix. Another test that was made was to set all albedo elements concerning the second moment flux  $\phi^{(2)}$  equal to zero (ie. rows and columns number 2 and 4).

reflective 

|   |   |   |   |   |   |   |   |   |
|---|---|---|---|---|---|---|---|---|
| 4 | 4 | 4 | 4 | 9 | 4 | 4 | 4 | 4 |
|---|---|---|---|---|---|---|---|---|

 water

**Figure 3.8** - The albedo example core, all nodes are 1 cm wide. The materials can be seen in Table 3.2.

The exact albedo matrix calculated with equation (3.29) was used in the tests to reduce errors due to approximations in the boundary condition.

# Chapter 4

## Results

In all graphs the dashed green lines are representing the node interfaces and all fluxes are normalized to the highest value of the fast average flux. The material numbers in the heterogeneous solution can be seen in Table 3.2 and in the homogeneous solution the material number is the calculated homogeneous cross-sections for each node calculated with equation (2.18) for the diffusion case and equation (2.19) for the SP3 case.

### 4.1 Heterogeneous solution

#### 4.1.1 Diffusion

The heterogeneous solution and the  $k_{eff}$  to the two examples solved with the diffusion equation can be seen in Figure 4.1.

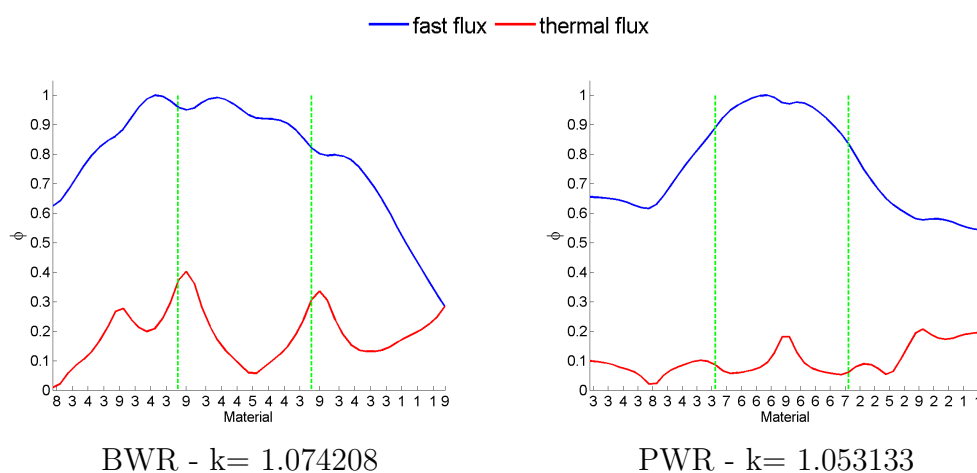
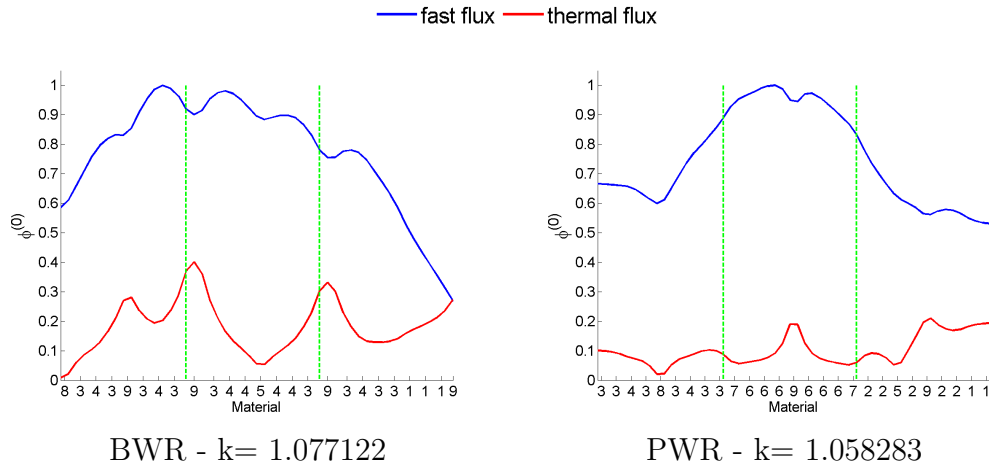


Figure 4.1 - Heterogeneous solution to the diffusion equation.

### 4.1.2 SP3

The heterogeneous solution to the two examples solved with the SP3 equations has two fluxes for each group. The integral flux  $\phi^{(0)}$  can be seen in Figure 4.2 and the second moment flux  $\phi^{(2)}$  can be seen in Figure 4.3.



**Figure 4.2** - Heterogeneous  $\phi^{(0)}$  solution to the SP3 equations.

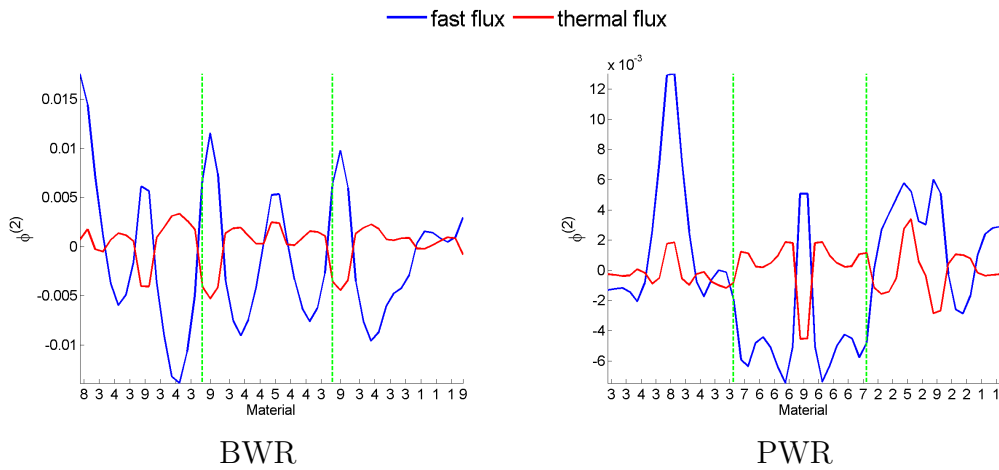


**Figure 4.3** - Heterogeneous  $\phi^{(2)}$  solution to the SP3 equations.

## 4.2 Homogeneous solution

There are two different ways to present the homogeneous solution, the calculated solution from the heterogeneous solution (Section 4.2.1) and the calculated solution with disconti-

nuity factors (Section 4.2.2).

## 4.2.1 Homogeneous solution from heterogeneous solution

The homogeneous flux calculated with equation (3.18) and the homogeneous interface flux calculated with equation (3.17) were calculated from the heterogeneous solution in Section 4.1. The heterogeneous interface fluxes were calculated from the heterogeneous solution with equation (3.7).

### 4.2.1.1 Diffusion

The average flux, heterogeneous and homogeneous interface fluxes calculated with the diffusion equation for the two examples can be seen in Figure 4.4.

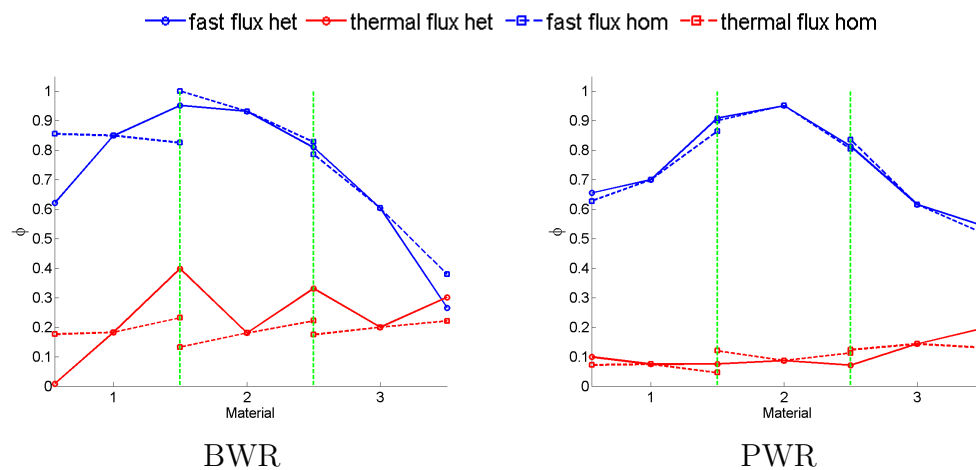


**Figure 4.4** - Homogeneous solution to the diffusion equation, with the heterogeneous and the homogeneous interface fluxes.

### 4.2.1.2 SP3

The average flux, heterogeneous and homogeneous interface fluxes calculated with the SP3 equations the two examples can be seen in Figure 4.5 for the integral flux and in Figure 4.6 for the second moment flux.

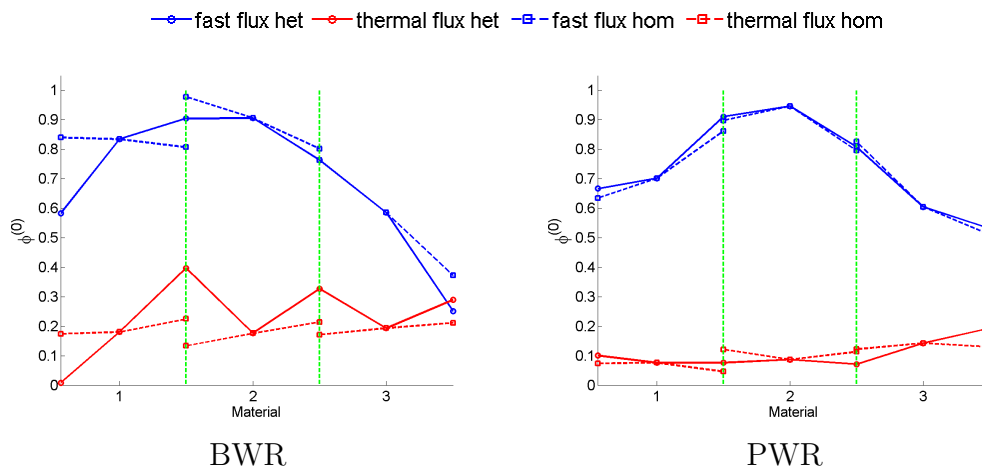


**Figure 4.5** - Homogeneous  $\phi^{(0)}$  solution to the SP3 equations, with the heterogeneous and the homogeneous interface fluxes.

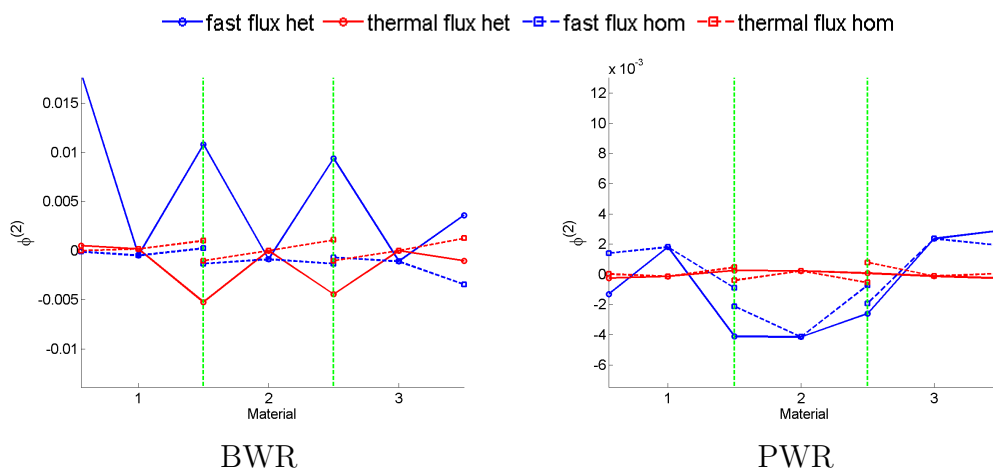


**Figure 4.6** - Homogeneous  $\phi^{(2)}$  solution to the SP3 equations, with the heterogeneous and the homogeneous interface fluxes.

### 4.2.2 Homogeneous solution from discontinuity factors

In Table 4.1 the methods that recreates the reaction rates and currents are marked with  $\checkmark$  and methods not working are marked with an X. Convergence means that the method converges to a set of unique discontinuity factors. System means that the discontinuity factors from that method were able to recreate reaction rates and interface currents. With recreate it means that the errors are in the same order of magnitude as the numerical accuracy of the solver.

**Table 4.1** - Working methods

| Method | Convergence |     | System    |     |
|--------|-------------|-----|-----------|-----|
|        | Diffusion   | SP3 | Diffusion | SP3 |
| 1      | ✓           | ✓   | ✓         | ✓   |
| 2      | ✓           | ✓   | ✓         | X   |
| 3      | ✓           | ✓   | ✓         | X   |
| 4.1    | X           | X   | ✓         | ✓   |
| 4.2    | ✓           | ✓   | ✓         | X   |

#### 4.2.2.1 Error calculations

The error calculations used the calculated homogeneous flux for different methods and the heterogeneous solution as the reference flux. There were two types of error calculations performed, the absolute error  $\varepsilon_{abs}$  defined as

$$\varepsilon_{abs} = \frac{\bar{\phi}^{hom} - \bar{\phi}^{het}}{\bar{\phi}_{system}^{het}} \quad (4.1)$$

and the relative error  $\varepsilon_{rel}$  defined as

$$\varepsilon_{rel} = \frac{\bar{\phi}^{hom} - \bar{\phi}^{het}}{\bar{\phi}^{het}} \quad (4.2)$$

The difference in  $k_{eff}$  was calculated as

$$\Delta k = k^{hom} - k^{het} \quad (4.3)$$

The errors calculated can be seen in Table 4.2 for the BWR example and in Table 4.3 for the PWR example. The “Diff - SP3” is the difference between the diffusion solution and the SP3 solution. In the rest of the rows in Table 4.2 the homogeneous SP3 equations are solved with different discontinuity factors. “ $f = 1$ ” no discontinuity factors are used and all are set to unity, “M 1” is the discontinuity factors from method 1, “M 2” is the discontinuity factors calculated by method 2, “M 3” is the discontinuity factors calculated by method 3, “M 4.1” is the discontinuity factors calculated by method 4 test 1, “M 4.2” is the discontinuity factors calculated by method 4 test 2. The last two are tested approximations where “M 1  $f^{(2)} = 1$ ” is the discontinuity factors from method 1 but with  $f^{(2)} = 1$  (not optimize as in method 2) and “ $f_{diff} f^{(2)} = 1$ ” uses the discontinuity factors calculated from the diffusion solution.

Note that  $\Delta k$  is in pcm =  $10^{-5}$  and by “0” means that the error is in the same order of magnitude as the accuracy required of the heterogeneous solver.

**Table 4.2** - Errors calculated with different discontinuity factors in BWR.

| Method                 | $\Delta k$ (pcm) | $\varepsilon_{abs,f}$ (%) | $\varepsilon_{rel,f}$ (%) | $\varepsilon_{abs,t}$ (%) | $\varepsilon_{rel,t}$ (%) |
|------------------------|------------------|---------------------------|---------------------------|---------------------------|---------------------------|
| Diff - SP3             | 291.4            | 0.47                      | 0.62                      | 0.84                      | 0.80                      |
| $f = 1$                | 529.8            | 11.25                     | 10.46                     | 5.33                      | 5.42                      |
| M 1                    | 0                | 0                         | 0                         | 0                         | 0                         |
| M 2                    | -10.1            | 0.12                      | 0.13                      | 0.17                      | 0.16                      |
| M 3                    | -990.1           | 4.6                       | 4.55                      | 3.97                      | 3.92                      |
| M 4.1                  | 0                | 0                         | 0                         | 0                         | 0                         |
| M 4.2                  | 19.1             | 0.004                     | 0.004                     | 0.03                      | 0.03                      |
| M 1 $f^{(2)} = 1$      | -1               | 0.02                      | 0.02                      | 0.04                      | 0.04                      |
| $f_{diff} f^{(2)} = 1$ | -10.0            | 0.20                      | 0.16                      | 0.02                      | 0.02                      |

**Table 4.3** - Errors calculated with different discontinuity factors in PWR.

| Method                 | $\Delta k$ (pcm) | $\varepsilon_{abs,f}$ (%) | $\varepsilon_{rel,f}$ (%) | $\varepsilon_{abs,t}$ (%) | $\varepsilon_{rel,t}$ (%) |
|------------------------|------------------|---------------------------|---------------------------|---------------------------|---------------------------|
| Diff - SP3             | 515.0            | -0.18                     | -0.16                     | -0.90                     | -0.84                     |
| $f = 1$                | 301.7            | 3.32                      | 3.90                      | 8.55                      | 9.16                      |
| M 1                    | 0                | 0                         | 0                         | 0                         | 0                         |
| M 2                    | 2.4              | -0.006                    | -0.005                    | -0.005                    | -0.005                    |
| M 3                    | -1558.4          | 11.02                     | 9.6                       | 9.15                      | 8.58                      |
| M 4.1                  | 0                | 0                         | 0                         | 0                         | 0                         |
| M 4.2                  | 2.4              | $<10^{-3}$                | $<10^{-3}$                | 0.004                     | 0.004                     |
| M 1 $f^{(2)} = 1$      | 4.3              | 0.01                      | 0.01                      | 0.03                      | 0.1                       |
| $f_{diff} f^{(2)} = 1$ | -2.5             | 0.02                      | 0.02                      | 0.08                      | 0.08                      |

#### 4.2.2.2 Discontinuity factors

The discontinuity factors from the working methods can be seen in Table 4.4 for the BWR example and in Table 4.5 for the PWR case. There is only one column for the diffusion equations since all used methods gave the same discontinuity factors. Since no unique set of discontinuity factors were found by method 4.1 no discontinuity factors will be presented. Where in the system the discontinuity are defined can be seen in Figure 3.3.

**Table 4.4** - Discontinuity factors for the working methods in the BWR example

|         | Diffusion |          | Method 1 |                |          |                |
|---------|-----------|----------|----------|----------------|----------|----------------|
|         | $\phi_f$  | $\phi_t$ | $\Phi_f$ | $\phi_f^{(2)}$ | $\Phi_t$ | $\phi_t^{(2)}$ |
| $f_1^-$ | 0.7255    | 0.0426   | 0.7364   | -162.9300      | 0.0500   | -813.7518      |
| $f_1^+$ | 1.1530    | 1.7178   | 1.1465   | 46.5164        | 1.7047   | -5.2163        |
| $f_2^-$ | 0.9513    | 3.0033   | 0.9500   | -8.0166        | 2.9389   | 5.0917         |
| $f_2^+$ | 0.9777    | 1.4939   | 0.9777   | -7.0534        | 1.4741   | -4.1254        |
| $f_3^-$ | 1.0298    | 1.8961   | 1.0274   | -13.3775       | 1.8819   | 4.2680         |
| $f_3^+$ | 0.7004    | 1.3615   | 0.7064   | -1.0458        | 1.3427   | -0.8265        |

**Table 4.5** - Discontinuity factors for the working methods in the PWR example

|         | Diffusion |          | Method 1 |                |          |                |
|---------|-----------|----------|----------|----------------|----------|----------------|
|         | $\phi_f$  | $\phi_t$ | $\Phi_f$ | $\phi_f^{(2)}$ | $\Phi_t$ | $\phi_t^{(2)}$ |
| $f_1^-$ | 1.0442    | 1.3770   | 1.0425   | -0.9368        | 1.3619   | -12.7854       |
| $f_1^+$ | 1.0515    | 1.6539   | 1.0490   | 4.5185         | 1.6201   | 0.5415         |
| $f_2^-$ | 1.0096    | 0.6300   | 1.0097   | 1.9397         | 0.6342   | -0.6210        |
| $f_2^+$ | 1.0108    | 0.6336   | 1.0110   | 3.5927         | 0.6378   | -0.1274        |
| $f_3^-$ | 0.9729    | 0.5773   | 0.9762   | 1.3475         | 0.5799   | 0.0875         |
| $f_3^+$ | 1.0488    | 1.5109   | 1.0437   | 1.5211         | 1.4877   | -4.9781        |

**Table 4.6** - Discontinuity factors for the non-working methods in the BWR example

|         | Method 2 |          | Method 3 |          | Method 4.2 |          |
|---------|----------|----------|----------|----------|------------|----------|
|         | $\Phi_f$ | $\Phi_t$ | $\Phi_f$ | $\Phi_t$ | $\Phi_f$   | $\Phi_t$ |
| $f_1^-$ | 0.7332   | 0.0500   | 0.7410   | 0.0492   | 0.6943     | 0.0441   |
| $f_1^+$ | 1.1408   | 1.7227   | 1.1355   | 1.7548   | 1.1161     | 1.7492   |
| $f_2^-$ | 0.9469   | 2.9871   | 0.9989   | 2.8952   | 0.9257     | 3.0133   |
| $f_2^+$ | 0.9737   | 1.4902   | 0.9121   | 1.4760   | 0.9535     | 1.5229   |
| $f_3^-$ | 1.0241   | 1.9027   | 1.2270   | 2.0935   | 0.9992     | 1.9362   |
| $f_3^+$ | 0.7020   | 1.3497   | 0.5148   | 1.2377   | 0.7286     | 1.3653   |

**Table 4.7** - Discontinuity factors for the non-working methods in the PWR example

|         | Method 2 |          | Method 3 |          | Method 4.2 |          |
|---------|----------|----------|----------|----------|------------|----------|
|         | $\Phi_f$ | $\Phi_t$ | $\Phi_f$ | $\Phi_t$ | $\Phi_f$   | $\Phi_t$ |
| $f_1^-$ | 1.0437   | 1.3612   | 0.9498   | 1.2779   | 1.0539     | 1.3736   |
| $f_1^+$ | 1.0499   | 1.6169   | 1.1650   | 1.7964   | 1.0552     | 1.6178   |
| $f_2^-$ | 1.0103   | 0.6323   | 1.0213   | 0.6454   | 1.0155     | 0.6292   |
| $f_2^+$ | 1.0116   | 0.6359   | 0.9355   | 0.6137   | 1.0148     | 0.6308   |
| $f_3^-$ | 0.9762   | 0.5804   | 1.1429   | 0.6701   | 0.9875     | 0.6256   |
| $f_3^+$ | 1.0434   | 1.4900   | 0.8938   | 1.3315   | 1.0675     | 1.4514   |

### 4.3 Albedo calculations

The calculated two group albedo matrix for diffusion theory can be seen in equation (4.4) and the albedo matrix for the SP3 equations in equation (4.5).

The calculated average fluxes when using albedo and nodes of water can be seen in the diffusion case in Figure 4.7. The SP3 calculations were calculated for two different cases, one with the calculated albedo matrix in equation (4.5) and one where rows 2, 4 and columns 2 and 4 in (4.5) is set to zero, these can be seen in Figure 4.8 and 4.9.

$$\underline{\mathbf{a}}_{diff} = \begin{bmatrix} 0.3829 & 0.0107 \\ 0.2472 & 0.8031 \end{bmatrix} \quad (4.4)$$

$$\underline{\mathbf{a}}_{SP3} = \begin{bmatrix} 0.2863 & -0.5334 & 0.0124 & 0.0093 \\ -0.1808 & -0.1397 & -0.0027 & -0.0019 \\ 0.2734 & 0.1817 & 0.7614 & -0.1850 \\ -0.0476 & -0.0288 & -0.2676 & -0.1983 \end{bmatrix} \quad (4.5)$$

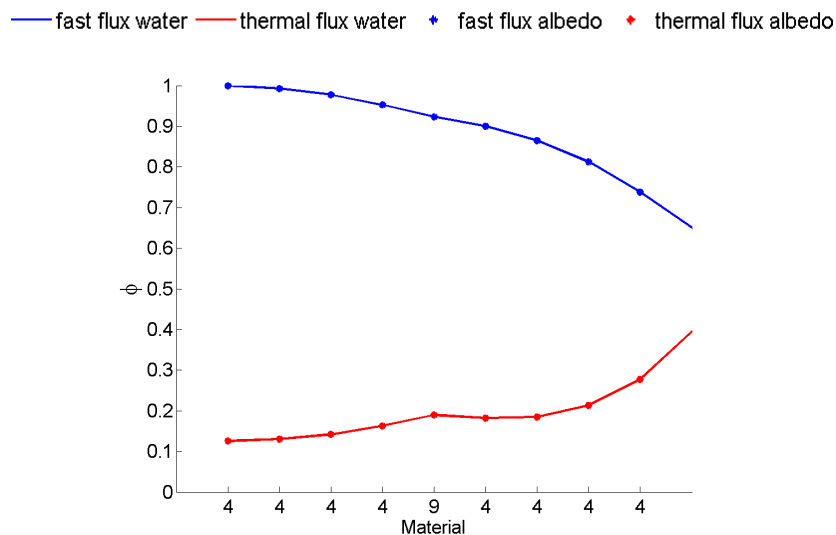


Figure 4.7 - The solution to the diffusion equation in the albedo test.

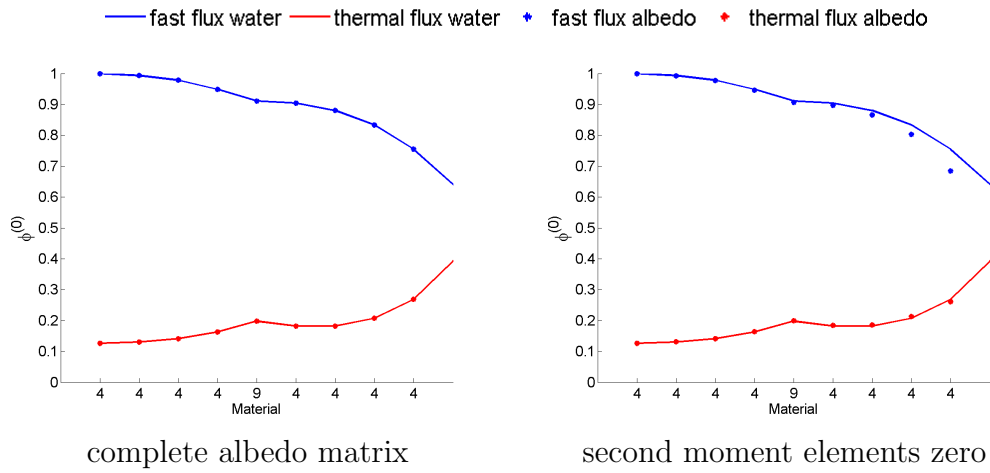


Figure 4.8 -  $\phi^{(0)}$  solution to the SP3 equations in the albedo test.

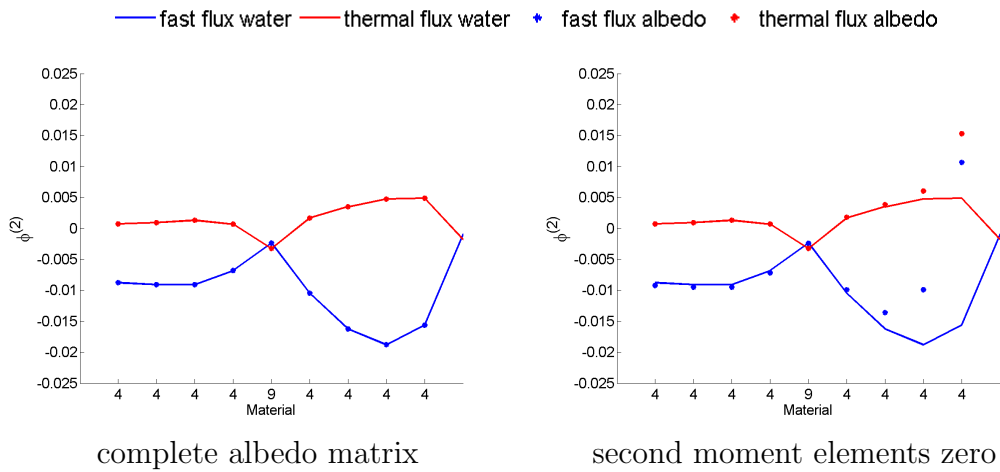


Figure 4.9 -  $\phi^{(2)}$  solution to the SP3 equations in the albedo test.

# Chapter 5

## Discussion

### 5.1 Result comparisons

When comparing the calculated errors in average flux and  $k_{eff}$  shown in Tables 4.2 and 4.3, the difference between diffusion theory and SP3 can be seen. The difference in  $k_{eff}$  is a couple of 100 pcm which is quite much. This difference can be expected since the differences in the average flux in Figure 4.1 and 4.2, where the SP3 solutions have more distinct changes with different materials than the diffusion solution as shown in [BL00].

The methods that recreated the solution (“M 1” and “M 4.1”) has “0” in all columns as they should since they recreates the heterogeneous solution. The second row “ $f = 1$ ” shows the result when no discontinuity factors are used and that result is not good.

Methods that did not recreate the solution but gave reasonable results were “M 2”, “M 1  $f^{(2)} = 1$ ”, “ $f_{diff} f^{(2)} = 1$ ” and “M 4.2”, all with reasonable errors in average flux and  $k_{eff}$ . Method 3 did not have any good result.

By comparing the discontinuity factors, Table 4.4 and 4.6 for the BWR system and 4.5 and 4.7 for the PWR system, one can see that all methods that gave similar results have similar discontinuity factors, as they should. But with method 3, which did not have any good results the discontinuity factors were quite different from the methods that gave better results, and no good solution can be expected.

### 5.2 Methods

The different methods derived to calculate the discontinuity factors were first tested if they were able to create discontinuity factors for the diffusion approximation. Since it is known that this is possible to do and if the solutions are unique all methods should give the same discontinuity factors, as all did except for method 4.1. With the SP3 approximation not all methods where able to create discontinuity factors that would work for the entire system as can be seen in Table 4.1.

Unfortunately the working methods have some drawbacks that will be discussed below.

### 5.2.1 Method 1

Method 1 worked as expected since it takes care of both fluxes the same way as in the diffusion case.

The problem with this method is that it works in theory but with implementation in a numerical code there can be problems. This is because the discontinuity factors for the second moment flux  $f^{(2)}$  vary a lot. As seen in Table 4.4 where the largest discontinuity factors have the value of

$$\begin{aligned} f_{1,f}^{(2)} &= -162.9300 \\ f_{1,t}^{(2)} &= -813.7518 \end{aligned} \tag{5.1}$$

These are rather big numbers compared with the discontinuity factors for the integral flux and it may not stop at a order of  $10^2$ .

The second order flux is small compared with the integral flux and both take positive and negative values as seen in Figure 4.3. This will make the average second order flux very small and may result in very small interface fluxes. This makes it possible to divide by very small numbers and even zero, which is not good from a numerical point of view.

To explain the large discontinuity factors for the second moment flux in equation (5.1) equation (3.17) can be studied. Since the boundary condition is set to reflective, the current will be zero. Then the only parameter determining the interface flux is the average flux, and the second order average flux is very small in this case, see Figure 4.6. This will result in a very small homogeneous interface flux.

**Variations of Method 1** The methods called “M 1  $f^{(2)} = 1$ ” and “ $f_{diff} f^{(2)} = 1$ ” in Table 4.3 and 4.2, did as expected not recreate the true solution, but had good results. Method “M 1  $f^{(2)} = 1$ ” can be used as a good approximation to discontinuity factors. By looking at Table 4.3 and 4.2 the “M 1  $f^{(2)} = 1$ ” gave very low errors in both examples.

### 5.2.2 Method 2

Method 2 was a method that did not recreate the solution. In the PWR example it had very good results (see Table 4.3) but not as good in the BWR example (see Table 4.2) which makes it a non-reliable method. The interesting thing is that the results without the optimization “M 1  $f^{(2)} = 1$ ” gave better results in both examples.

It was found out that the average flux was not needed for the optimization in method 2, this is because the material matrices and the currents will give the average flux.

### 5.2.3 Method 4

When looking at the entire system and just recreating the currents and average fluxes (method 4.1), the method found one set of discontinuity factors that recreated the conservation equations (2.20) and (2.21) for each start guess, this was the result for both diffusion

theory and SP3 theory. This problem can be explained by calculating the number of parameters and unknown. There are  $2n + 1$  parameters and  $2n$  unknowns ( $n$  is the number of nodes). The problem is that the parameters (reaction rates and currents) are coupled, and therefore it will be an underdetermined system with an infinite number of solutions.

The second test in method 4 was to include the interface fluxes as a parameter. Then the solver found one unique set of discontinuity factors regardless of the start guess, this was the result for both diffusion theory and SP3 theory. The difference was that in the diffusion case, the solver converged to the same discontinuity factors as in the other methods and recreated the system. This was not the case in the SP3 case, where the solution was not recreated.

Both these problems rise because of the interface flux. The reason why the discontinuity factors are introduced in the first place is to handle the discontinuities in the interface flux, but in method 4 the discontinuity factors are redefined and therefore all parameters (currents, reaction rates and interface fluxes) cannot be conserved when  $f^{(2)} = 1$  with the definitions made in this thesis.

### 5.3 Albedo calculation

For the albedo calculation an explicit formula for the albedo was derived (equation (3.29)) and should thereby give the same result as if there were water nodes present in the calculation instead. This can be seen in Figures 4.7, 4.8 and 4.9.

By comparing the albedo matrix for diffusion theory (equation (4.4)) and SP3 theory (equation (4.5)), the difference between the corresponding elements are quite similar.

If all elements concerning the second order flux are set to zero there will be a big change in the second moment flux (see Figure 4.9) and it will affect the integral flux. One should also keep in mind that the albedo matrix is constructed for  $\Phi$  and not  $\phi^{(0)}$  which is the corresponding flux to the flux calculated from the diffusion equation, and small differences are expected.

# Chapter 6

## Conclusion and Future work

This thesis has shown that it is possible to use discontinuity factors in SP3 theory in a number of ways, either as an approximation or to recreate the heterogeneous solution exact. To be able to recreate the solution there has to be a sacrifice either by numerical instabilities or no unique solution, non-practical in any computer code. It was also shown in method 4.2 that recreating the system, reaction rates, currents and interface fluxes, with  $f^{(2)} = 1$  is not possible with only discontinuity factors.

The best approximation to use discontinuity factors in SP3 found in this thesis, was to use  $f^{(0)}$  defined with  $\Phi$  and use  $f^{(2)} = 1$ , which gave very small errors in both examined examples.

To be able to recreate the reaction rates, currents and interface fluxes for the integral flux, future improvements are needed. The next thing to look at and change is the definition of the homogeneous cross-section. This may result in the recreation of the system and numerical stabilities.

# Bibliography

- [BL00] P. S. Brantley and E. W. Larsen. The simplified  $P_3$  approximation. *Nucl. Sci. Eng.*, 134:1–21, 2000.
- [BRL95] D. Biswas, S. Rathbun, and S.Y. Lee. Weapons-grade plutonium dispersion in pressurized water reactor. *Nucl. Sci. Eng.*, 121:1, 1995.
- [Cha11] J Chang. Table of Nuclides, KAERI(korea atomic energy research institute), Feb 2011. <http://atom.kaeri.re.kr/>.
- [CLR02] G. Choppin, J-O. Liljenzin, and J. Rydberg. *Radiochemistry and Nuclear Chemistry, Third Edition*. Butterworth-Heinemann, 2002.
- [Dem09] C. Demazière. *Physics of Nuclear Reactors*. Chalmers University of Technology, 2009.
- [Dem10] C. Demazière. *Modelling of nuclear reactors*. Chalmers University of Technology, 2010.
- [FCM95] P. Fougeras, S. Cathalau, and J. Mondot. Optimization of a calculation scheme for the treatment of plutonium recycling in pressurized water reactors. *Nucl. Sci. Eng.*, 121:32, 1995.
- [Lin11] Sten-Örjan. Lindahl. Personal communication, 2011.
- [LMM96] E.W. Larsen, J.E. Morel, and J.M. McGhee. Asymptotic derivation of the multi-group  $P_1$  and simplified  $P_N$  equations with anisotropic scattering. *Nucl. Sci. Eng.*, 123:328–342, 1996.
- [Sca11] Studsvik Scandpower. Homepage, May 2011. <http://www.studsvikscandpower.com>.
- [Tre06] H.R. Trellue. Safety and neutronics: A comparison of MOX vs UO<sub>2</sub> fuel. *Prog. Nucl. Energy*, 48(I2):135–145, 2006.

# Appendix A

## Matrix form of transport equations

As mentioned in Section 2.1.3.2 and 2.1.3.1 the diffusion equation and SP3 equations can be written in matrix form as

$$\underline{\mathbf{D}} \frac{\partial^2}{\partial x^2} \phi + \underline{\Sigma} \phi = 0 \quad (\text{A.1})$$

The matrices for this equation will be written for two groups in the following sections

### A.1 Diffusion

In the diffusion case the matrices will look as following

$$\underline{\mathbf{D}} = \begin{bmatrix} D_f & 0 \\ 0 & D_t \end{bmatrix}, \quad \phi = \begin{bmatrix} \phi_f \\ \phi_t \end{bmatrix}, \quad \underline{\Sigma} = \underline{\Sigma}_a + \underline{\Sigma}_s + \frac{1}{k_{eff}} \underline{\Sigma}_f \quad (\text{A.2})$$

$$\underline{\Sigma}_a = - \begin{bmatrix} \Sigma_{a,f} & 0 \\ 0 & \Sigma_{a,t} \end{bmatrix}, \quad \underline{\Sigma}_s = \begin{bmatrix} -\Sigma_{s,tf} & \Sigma_{s,ft} \\ \Sigma_{s,tf} & -\Sigma_{s,ft} \end{bmatrix}, \quad \underline{\Sigma}_f = \begin{bmatrix} \Sigma_{f,f} & \Sigma_{f,t} \\ 0 & 0 \end{bmatrix} \quad (\text{A.3})$$

### A.2 SP3

The four coupled SP3 equations will in matrix form look as

$$\underline{\mathbf{D}} = \begin{bmatrix} D_{1,f} & 0 & 0 & 0 \\ 0 & D_{3,t} & 0 & 0 \\ 0 & 0 & D_{1,t} & 0 \\ 0 & 0 & 0 & D_{3,t} \end{bmatrix}, \quad \phi = \begin{bmatrix} \Phi_f \\ \phi_f^{(2)} \\ \Phi_t \\ \phi_t^{(2)} \end{bmatrix}, \quad \underline{\Sigma} = \underline{\Sigma}_s + \underline{\Sigma}_r + \frac{1}{k_{eff}} \underline{\Sigma}_f \quad (\text{A.4})$$

where

$$\Phi_g = \phi_g^{(0)} + 2\phi_g^{(2)} \quad (\text{A.5})$$

and

$$\underline{\Sigma}_s = \begin{bmatrix} 0 & 0 & \Sigma_{s,ft} & -2\Sigma_{s,ft} \\ 0 & 0 & -\frac{2}{3}\Sigma_{s,ft} & \frac{4}{3}\Sigma_{s,ft} \\ \Sigma_{s,t,f} & -2\Sigma_{s,t,f} & 0 & 0 \\ -\frac{2}{3}\Sigma_{s,t,f} & \frac{4}{3}\Sigma_{s,t,f} & 0 & 0 \end{bmatrix} \quad (\text{A.6})$$

$$\underline{\Sigma}_r = - \begin{bmatrix} \Sigma_{r1,f} & -2\Sigma_{r1,f} & 0 & 0 \\ -\frac{2}{3}\Sigma_{r1,f} & \frac{4}{3}\Sigma_{r1,f} + \Sigma_{r3,f} & 0 & 0 \\ 0 & 0 & \Sigma_{r1,t} & -2\Sigma_{r1,t} \\ 0 & 0 & -\frac{2}{3}\Sigma_{r1,t} & \frac{4}{3}\Sigma_{r1,t} + \Sigma_{r3,t} \end{bmatrix} \quad (\text{A.7})$$

$$\underline{\Sigma}_f = \begin{bmatrix} \nu_f \Sigma_{f,f} & -2\nu_f \Sigma_{f,f} & \nu_t \Sigma_{f,t} & -2\nu_t \Sigma_{f,t} \\ -\frac{2}{3}\nu_f \Sigma_{f,f} & \frac{4}{3}\nu_f \Sigma_{f,f} & -\frac{2}{3}\nu_t \Sigma_{f,t} & \frac{4}{3}\nu_t \Sigma_{f,t} \\ 0 & 0 & 0 & 0 \\ 0 & 0 & 0 & 0 \end{bmatrix} \quad (\text{A.8})$$

# Appendix B

## Derivations

This following appendix contains longer derivations for better understanding of the different methods. The method used to solve the matrix equations was gotten from [Lin11].

### B.1 Nodal solution with known average flux and currents

Both the diffusion equation and the SP3 equations for a homogeneous, one dimensional node with  $\frac{-h}{2} < x < \frac{h}{2}$  can be written in matrix form as

$$\underline{D} \frac{\partial^2}{\partial x^2} \phi(x) + \underline{\Sigma} \phi(x) = 0 \quad (\text{B.1})$$

and can be rewritten as

$$\frac{\partial^2}{\partial x^2} \phi(x) + \underline{D}^{-1} \underline{\Sigma} \phi(x) = 0 \quad (\text{B.2})$$

By calculating the eigenvalues and eigenvector of the buckling matrix  $\underline{B}^2 = \underline{D}^{-1} \underline{\Sigma}$  as

$$B_i^2 \underline{U}_i = \underline{B}^2 \underline{U}_i \quad (\text{B.3})$$

With all eigenvectors  $\underline{U}_i$  in a matrix  $\underline{U}$  it can be used as a transformation matrix, and multiply equation (B.1) with  $\underline{U}^{-1}$  the new equation

$$\frac{\partial^2}{\partial \xi^2} \psi(\xi) + \underline{b}^2 \psi(\xi) = 0 \quad (\text{B.4})$$

can be obtained, where

$$\psi = \underline{U}^{-1} \phi \quad (\text{B.5})$$

$$b_i^2 = \frac{1}{4} h^2 B_i^2 \quad (\text{B.6})$$

$$\xi = \frac{2x}{h} : -1 < \xi < 1 \quad (\text{B.7})$$

Equation (B.4) now contains  $i$  number of uncoupled equations. Each equation can be written as

$$\frac{\partial^2}{\partial \xi^2} \psi_i + b_i^2 \psi_i = 0 \quad (\text{B.8})$$

The general solution to (B.8) can be written as

$$\psi_i(\xi) = A_i \cos(b_i \xi) + B_i \sin(b_i \xi) \quad (\text{B.9})$$

Assume known side gradients defined as

$$\begin{aligned} g_i^- &= -\frac{\partial \psi_i}{\partial \xi}(-1) \\ g_i^+ &= \frac{\partial \psi_i}{\partial \xi}(1) \end{aligned} \quad (\text{B.10})$$

and the average flux is defined as

$$\bar{\psi}_i = \frac{1}{2} \int_{-1}^1 \psi_i(\xi) d\xi \quad (\text{B.11})$$

evaluating equations (B.10) gives

$$\begin{aligned} g_i^- &= -A_i b_i \sin(b_i) - B_i b_i \cos(b_i) \\ g_i^+ &= -A_i b_i \sin(b_i) + B_i b_i \cos(b_i) \end{aligned} \quad (\text{B.12})$$

By subtraction of equations (B.12) a new quantity can be defined

$$\begin{aligned} \tilde{g}_i &= g_i^+ - g_i^- \\ &= 2B_i b_i \cos(b_i) \end{aligned} \quad (\text{B.13})$$

with the average flux (B.11) calculated

$$\bar{\psi}_i = \frac{A_i}{b_i} \sin(b_i) \quad (\text{B.14})$$

From equations (B.14) and (B.13) constants  $A_i$  and  $B_i$  can be calculated to

$$A_i = \bar{\psi}_i \frac{b_i}{\sin(b_i)} \quad (\text{B.15})$$

$$B_i = \frac{\tilde{g}_i}{2b_i \cos(b_i)} \quad (\text{B.16})$$

and  $\psi_i$  finally becomes

$$\psi_i(\xi) = \bar{\psi} \frac{b_i}{\sin(b_i)} \cos(b_i \xi) + \frac{\tilde{g}}{2b_i \cos(b_i)} \sin(b_i \xi) \quad (\text{B.17})$$

The interface fluxes can then be calculated according to

$$\psi_i^- = \psi_i(-1) = \frac{\bar{\psi}_i}{\Lambda} - \frac{\tilde{g}_i}{2} \Lambda \quad (\text{B.18})$$

$$\psi_i^+ = \psi_i(1) = \frac{\bar{\psi}_i}{\Lambda} + \frac{\tilde{g}_i}{2} \Lambda \quad (\text{B.19})$$

with

$$\Lambda = \frac{\tan(b_i)}{b_i} \quad (\text{B.20})$$

The modal gradient can be calculated to

$$g_i^+ = \frac{\tilde{g}_i}{2} - \bar{\psi}_i b_i^2 \quad (\text{B.21})$$

Using the interface flux in equation (B.19),  $\tilde{g}_i$  can be substituted from equation (B.21) and the result will be

$$g_i^+ = \frac{1}{2} \left( \frac{2}{\Lambda} \psi_i^+ - \frac{2}{\Lambda^2} \bar{\psi}_i \right) - \bar{\psi}_i b_i^2 \quad (\text{B.22})$$

After some trigonometric formulas the final relation for the side gradient becomes

$$g_i^+ = t_i(\psi_i^+ - s_i \bar{\psi}_i) \quad (\text{B.23})$$

where

$$t_i = \frac{b_i}{\tan(b_i)} \quad (\text{B.24})$$

$$s_i = \frac{2b_i}{\sin(2b_i)} \quad (\text{B.25})$$

To go back to ordinary neutron current  $J$  the solutions are multiplied by the transformation matrix  $\underline{U}$  and by  $-\frac{2}{h}\underline{D}$

$$\mathbf{J}^+ = -\underline{\mathbf{d}}(\boldsymbol{\phi}^+ - \underline{\mathbf{s}}\bar{\boldsymbol{\phi}}) \quad (\text{B.26})$$

where

$$\underline{\mathbf{d}} = \frac{2}{h}\underline{\mathbf{D}}\underline{\mathbf{U}} \begin{bmatrix} t_1 & & 0 \\ & \ddots & \\ 0 & & t_G \end{bmatrix} \underline{\mathbf{U}}^{-1} \quad (\text{B.27})$$

$$\underline{\mathbf{s}} = \underline{\mathbf{U}} \begin{bmatrix} s_1 & & 0 \\ & \ddots & \\ 0 & & s_G \end{bmatrix} \underline{\mathbf{U}}^{-1}$$

By using the fact that the neutron current and the flux needs to be continuous at the interfaces a relation regarding the current between two nodes and the interface flux can be derived as

$$J_{n \rightarrow m} = \underline{C}_{nm} \bar{\phi}_n - \underline{C}_{mn} \bar{\phi}_m \quad (\text{B.28})$$

$$\phi_{nm} = \underline{d}_m^{-1} \underline{C}_{nm} \bar{\phi}_n - \underline{d}_n^{-1} \underline{C}_{mn} \bar{\phi}_m \quad (\text{B.29})$$

where

$$\underline{C}_{nm} = (\underline{d}_n^{-1} + \underline{d}_m^{-1})^{-1} \underline{s}_n \quad (\text{B.30})$$

## B.2 Nodal solution with known interface fluxes

When solving with known interface flux the same procedure will be used. Therefore the general solution will be on the form as in equation (B.9). This time the assumed boundary conditions are

$$\begin{aligned} \psi_i(-1) &= \psi_i^- = A_i \cos(b_i) - B_i \sin(b_i) \\ \psi_i(1) &= \psi_i^+ = A_i \cos(b_i) + B_i \sin(b_i) \end{aligned} \quad (\text{B.31})$$

$A_i$  and  $B_i$  is now found from equation (B.31)

$$A_i = \frac{\psi_i^- + \psi_i^+}{2 \cos(b_i)} \quad (\text{B.32})$$

$$B_i = \frac{\psi_i^+ - \psi_i^-}{2 \sin(b_i)} \quad (\text{B.33})$$

to get the modal gradient, equation (B.9) is differentiated

$$\frac{\partial \psi_i}{\partial \xi} = g(\xi) = -A_i b_i \sin(b_i \xi) + B_i b_i \cos(b_i \xi) \quad (\text{B.34})$$

then the modal gradient at the boundaries can be calculated

$$g(-1)_i = g_i^- = \psi_i^- \left( \frac{b_i \tan(b_i)}{2} - \frac{b_i}{2 \tan(b_i)} \right) + \psi_i^+ \left( \frac{b_i \tan(b_i)}{2} + \frac{b_i}{2 \tan(b_i)} \right) \quad (\text{B.35})$$

$$g(1)_i = g_i^+ = \psi_i^- \left( -\frac{b_i \tan(b_i)}{2} - \frac{b_i}{2 \tan(b_i)} \right) + \psi_i^+ \left( -\frac{b_i \tan(b_i)}{2} + \frac{b_i}{2 \tan(b_i)} \right) \quad (\text{B.36})$$

and the average flux can be calculated

$$\bar{\psi}_i = \frac{1}{2} \int_{-1}^1 \psi_i d\xi = \frac{\psi_i^- + \psi_i^+}{2b_i} \tan(b_i) \quad (\text{B.37})$$

To make this manageable new quantities are introduced

$$c_{I,i}^- = \frac{b_i \tan(b_i)}{2} - \frac{b_i}{2 \tan(b_i)} \quad (\text{B.38})$$

$$c_{I,i}^+ = \frac{b_i \tan(b_i)}{2} + \frac{b_i}{2 \tan(b_i)} \quad (\text{B.39})$$

$$c_{II,i}^- = -\frac{b_i \tan(b_i)}{2} - \frac{b_i}{2 \tan(b_i)} \quad (\text{B.40})$$

$$c_{II,i}^+ = -\frac{b_i \tan(b_i)}{2} + \frac{b_i}{2 \tan(b_i)} \quad (\text{B.41})$$

$$M_i = \frac{\tan(b_i)}{2b_i} \quad (\text{B.42})$$

Then equation (B.37) and (B.35) can be rewritten as

$$\begin{aligned} g_i^- &= c_{I,i}^- \psi_i^- + c_{I,i}^+ \psi_i^+ \\ g_i^+ &= c_{II,i}^- \psi_i^- + c_{II,i}^+ \psi_i^+ \\ \bar{\psi}_i &= M_i (\psi_i^- + \psi_i^+) \end{aligned} \quad (\text{B.43})$$

To transform back to the real flux and current equation (B.43) is multiplied with the transformation matrix  $\underline{U}$  and in the current case a factor  $-\frac{2}{h}\underline{D}$  needs to be multiplied (as in equation (B.26))

The expression for the current and the average flux will then become

$$\underline{J}^\pm = \frac{2}{h} \underline{D}^* \underline{C} \underline{U}^* \phi_s \quad (\text{B.44})$$

$$\bar{\phi} = \underline{U} \underline{M}^* \underline{U}^* \phi_s \quad (\text{B.45})$$

where

$$\begin{aligned}
\mathbf{J}^\pm &= \begin{bmatrix} J_1^- \\ \vdots \\ J_G^- \\ J_1^+ \\ \vdots \\ J_G^+ \end{bmatrix}, \quad \underline{\mathbf{D}}^* = \begin{bmatrix} \underline{\mathbf{D}} & \underline{\mathbf{0}} \\ \underline{\mathbf{0}} & \underline{\mathbf{D}} \end{bmatrix}, \quad \underline{\mathbf{C}} = \begin{bmatrix} c_{I,1}^- & 0 & c_{I,1}^+ & 0 \\ & \ddots & & \ddots \\ 0 & & c_{I,G}^- & c_{I,G}^+ \\ c_{II,1}^- & & 0 & c_{II,1}^+ \\ & \ddots & & \ddots \\ 0 & & c_{II,G}^- & c_{II,G}^+ \end{bmatrix} \\
\underline{\mathbf{M}}^* &= \begin{bmatrix} M_1 & 0 & M_1 & 0 \\ & \ddots & & \ddots \\ 0 & & M_G & M_G \end{bmatrix}, \quad \underline{\mathbf{U}}^* = \begin{bmatrix} \underline{\mathbf{U}}^{-1} & \underline{\mathbf{0}} \\ \underline{\mathbf{0}} & \underline{\mathbf{U}}^{-1} \end{bmatrix}, \quad \phi_s = \begin{bmatrix} \phi_1^- \\ \vdots \\ \phi_G^- \\ \phi_1^+ \\ \vdots \\ \phi_G^+ \end{bmatrix}
\end{aligned} \tag{B.46}$$

### B.3 Albedo tests

To be able to calculate the albedo matrix for an infinite half slab made up of water, the following system needs to be solved

$$\begin{aligned}
\underline{\mathbf{D}} \frac{d^2}{dx^2} \phi(x) - \underline{\Sigma} \phi(x) &= 0 \\
0 < x < \infty & \\
-\underline{\mathbf{D}} \frac{d}{dx} \phi(0) &= \mathbf{J}
\end{aligned} \tag{B.47}$$

To get the albedo into the problem the following relations are used

$$\mathbf{j}^{in} = \underline{\mathbf{a}} \mathbf{j}^{out} \tag{B.48}$$

$$\mathbf{J} = \mathbf{j}^{out} - \mathbf{j}^{in} \tag{B.49}$$

$$\tag{B.50}$$

By substituting  $\mathbf{j}^{in}$  we get

$$\mathbf{J} = (\underline{\mathbf{I}} - \underline{\mathbf{a}}) \mathbf{j}^{out} \tag{B.51}$$

To solve the system in (B.47) the same method as in Section B.1 and the eigenvalues and eigenvectors are obtained as in equation (B.3) and (B.4). To transform the boundary condition the current is multiplied by  $\underline{\mathbf{D}}^{-1}$  and the transformation matrix  $\underline{\mathbf{U}}^{-1}$  and the new non-coupled system is found as

$$\begin{aligned}\frac{d^2}{dx^2}\psi_i(x) - B_i^2\phi(x) &= 0 \\ 0 < x < \infty \\ \frac{d}{dx}\psi_i &= [\underline{U}^{-1}\underline{D}^{-1}\underline{J}]_i\end{aligned}\tag{B.52}$$

Equation (B.52) has the general solution

$$\psi = A_1e^{B_ix} + A_2e^{-B_ix}\tag{B.53}$$

Since a limited solution is sought  $A_1 = 0$  and  $A_2$  is found from the boundary condition

$$A_2 = \frac{1}{B_i}[\underline{U}^{-1}\underline{D}^{-1}\underline{J}]_i\tag{B.54}$$

with the boundary  $x = 0$  the relation for the flux is given by multiplying  $\psi_i(0)$  with  $\underline{U}$  and get

$$\phi_s = \underline{U}\underline{b}\underline{U}^{-1}\underline{D}^{-1}\underline{J}\tag{B.55}$$

where

$$\underline{b} = \begin{bmatrix} \frac{1}{B_1} & & 0 \\ & \ddots & \\ 0 & & \frac{1}{B_G} \end{bmatrix}\tag{B.56}$$

With the interface flux it is possible use the definition of the partial currents for diffusion [Dem10]

$$\mathbf{j}^{out} = \frac{1}{4}\phi^- + \frac{1}{2}\underline{J}\tag{B.57}$$

and for SP3 [BL00]

$$\begin{aligned}j_1^{out} &= \frac{1}{4}\Phi_s + \frac{1}{2}J_1 - \frac{11}{16}\phi_s^{(2)} \\ j_3^{out} &= \frac{7}{16}\phi_s^{(2)} + \frac{1}{2}J_3 - \frac{1}{16}\Phi_s\end{aligned}\tag{B.58}$$

These can be rewritten to matrix form as

$$\mathbf{j}^{out} = \underline{\mathbf{G}}\phi_s - \frac{1}{2}\underline{\mathbf{I}}\underline{\mathbf{J}}\tag{B.59}$$

where

$$\begin{aligned}\underline{\mathbf{G}}_g &= \begin{bmatrix} \frac{1}{4} & -\frac{11}{16} \\ -\frac{1}{16} & \frac{7}{16} \end{bmatrix} \\ \underline{\mathbf{G}}_{diff} &= \text{diag}(\frac{1}{4}) \\ \underline{\mathbf{G}}_{SP3} &= \text{diag}(\underline{\mathbf{G}}_g)\end{aligned}\tag{B.60}$$

by combining equations (B.51), (B.55) and (B.59) the following relation is found

$$\mathbf{j}^{out} = \underline{\mathbf{G}}\underline{\mathbf{U}}\underline{\mathbf{b}}\underline{\mathbf{U}}^{-1}\underline{\mathbf{D}}^{-1}(\underline{\mathbf{I}} - \underline{\mathbf{a}})\mathbf{j}^{out} - \frac{1}{2}\underline{\mathbf{I}}(\underline{\mathbf{I}} - \underline{\mathbf{a}})\mathbf{j}^{out} \quad (\text{B.61})$$

and by some manipulations the final expression for the albedo matrix is given by

$$\underline{\mathbf{a}} = -(\underline{\mathbf{G}}\underline{\mathbf{U}}\underline{\mathbf{b}}\underline{\mathbf{U}}^{-1}\underline{\mathbf{D}}^{-1} + \frac{1}{2}\underline{\mathbf{I}})^{-1}(\frac{1}{2}\underline{\mathbf{I}} - \underline{\mathbf{G}}\underline{\mathbf{U}}\underline{\mathbf{b}}\underline{\mathbf{U}}^{-1}\underline{\mathbf{D}}^{-1}) \quad (\text{B.62})$$